MECHANISMS OF IMPAIRED OSTEOBLAST FUNCTION DURING DISUSE

A Dissertation

by

MATTHEW ROBERT ALLEN

Submitted to the Office of Graduate Studies of
Texas A&M University
in partial fulfillment of the requirements for the degree of

DOCTOR OF PHILOSOPHY

August 2003

Major Subject: Kinesiology

MECHANISMS OF IMPAIRED OSTEOBLAST FUNCTION DURING DISUSE

A Dissertation

by

MATTHEW ROBERT ALLEN

Submitted to Texas A&M University
in partial fulfillment of the requirements
for the degree of

DOCTOR OF PHILOSOPHY

Approved as to style and content by:

Susan A. Bloomfield (Chair of Committee)	Michael D. Delp (Member)
Harry A. Hogan (Member)	Robert B. Armstrong (Member)
Steven Dorman (Head of Department)	

August 2003

Major Subject: Kinesiology

ABSTRACT

Mechanisms of Impaired Osteoblast Function During Disuse.

(August 2003)

Matthew Robert Allen, B.S., Alma College

Chair of Advisory Committee: Dr. Susan A. Bloomfield

Prolonged periods of non-weightbearing activity result in a significant loss of bone mass which increases the risk of fracture with the initiation of mechanical loading. The loss of bone mass is partially driven by declines in bone formation yet the mechanisms responsible for this decline are unclear. To investigate the limitations of osteoblasts during disuse, marrow ablation was superimposed on hindlimb unloaded mice. Marrow ablation is a useful model to study osteoblast functionality as new cancellous bone is rapidly formed throughout the marrow of a long bone while hindlimb unloading is the most common method used to produce skeletal unloading. The specific hypotheses of this study were aimed at determining if changes in osteoblast functionality, differentiation, and/or proliferation were compromised in non-weightbearing bone in response to a bone formation stimulus. Additionally, the influence of having compromised osteoblast functionality at the time of stimulation was assessed in non-weightbearing bones. Key outcome measures used to address these hypotheses included static and dynamic cancellous bone histomorphometry, bone densitometry, and real-time polymerase chain reaction (PCR) analyses of gene expression. The results document similar ablation-induced increases of cancellous bone

in both weightbearing and unloaded animals. Similarly, there was no influence of load on ablation-induced increases in cancellous bone forming surface or mineral apposition rate. Unloading did significantly attenuate the ablation-induced increase in bone formation rate, due to reduced levels of total surface mineralization. When osteoblast functionality was compromised prior to marrow ablation, bone formation rate increases were also attenuated in ablated animals due to reduced mineralization. Additionally, increases in forming surface were attenuated as compared to unloaded animals having normal osteoblast function at the time of ablation. Collectively, these data identify mineralization as the limiting step in new bone formation during periods of disuse. The caveat, however, is that when bone formation is stimulated after a period of unloading sufficient to compromise osteoblast functionality, increases in osteoblast recruitment to the bone surface are compromised.

DEDICATION

This work is unequivocally dedicated to Kristine, my wife and best friend. I have never loved, nor ever will love another as much as I love her. Through the physical and mental challenges of graduate school, whether 1,400 miles away or by my side, she has provided unwavering support of me and all of my endeavors. More important, however, are the selfless sacrifices she has made in order that I may pursue a career that I love. Without this support or these sacrifices on her part, this body of work would never have been possible. I pray that I can provide the same steadfast support for her dreams throughout all the days of our life together.

ACKNOWLEDGMENTS

I would like to thank the following individuals who have contributed to my being able to produce this body of work. Without their help this document would not have been possible.

First and foremost, to Sue, for taking a chance on a young and eager "Scot", who was by no means a standout with respect to the traditional measures of scholarly aptitude. She has provided me with invaluable lessens in scientific and professional conduct while simultaneously helping me to build a network within the community of skeletal scientists. For considering me as not just a student, but as a collaborator in much of her work, and for allowing me opportunities that are rare for most graduate students, I am forever grateful.

To Mike, for the friendship, listening ear, and advice which he has provided over the years. For the wonderful opportunity to work alongside him on the STS-107 mission, a once in a lifetime opportunity from which I gained a greater perspective on many fronts. Most of all, however, I am grateful for the openness and honesty that he has shown me and for being a role model. His passion toward the science he performs and the students he mentors is inspiring. I hope my productivity as a scientist, a researcher, and a teacher can someday equal his.

To Harry, for always providing a listening ear, whether it be to discuss data or life, even when it meant delaying important work until 3:00 am. His dedication to teaching, both in and out of the classroom, is something I will always strive to replicate.

His friendship has meant, and will continue to mean, the world to me (as will his obsession with Krispy Kremes).

To Bob, for being an ever present role model in scientific integrity and professional conduct. Throughout my scientific career, I can only hope to interact with professionals with a fraction of the integrity that Dr. A possesses.

To "Dr." Jan Stafinsky/Stallone, for being an unwavering presence in the laboratory. She helped me maintain my sanity on days too numerous to count, and put up with my day-to-day moodiness. This is a true feat, as she surely saw me as much or more than Kristine over the years, yet took no vow requiring her to put up with me!

To Dr. John Davis, for providing me the avenue to purse my dreams in graduate school. Without his personal guidance, support, and recommendations, I would never be where I am today. He is a model for what all liberal arts professor should be. Even beyond that, he is a true and consummate friend.

To Dr. Larry Lawhorne, for introducing me to the field of bone physiology through his ultimatum of studying osteoporosis or glaucoma during my summer fellowship at the Michigan Masonic Home.

To my mom and dad, two of my largest supporters and greatest role models. They have taught me more than all the others combined because no matter how hard one works, or what one achieves, how one carries oneself is most important. I am what I am today because of the way I was raised, and pray I am half the parent to my children that they have been to me.

Most importantly, I must acknowledge the real presence of God in my life over the past three years. Through joining the Catholic Church, I have gained a spirituality that has filled a large void in my life. I have come to realize a faith greater than I ever knew existed and know that, through Him, I have received the strength to accomplish what I have to this point. For the Glory of God, I present this body of work in hopes that it will, in some small way, better mankind.

The Unknown

As we know,

There are known knowns.

There are things we know we know.

We also know

There are known unknowns.

That is to say

We know there are some things

We do not know.

But there are also unknown unknowns,

The ones we don't know

We don't know.

—D.H. Rumsfeld, Feb. 12, 2002

TABLE OF CONTENTS

LIST OF FIGURES

LIST OF TABLES

CHAPTER I

INTRODUCTION

The relationship between mechanical loading and bone mass can be traced back to the pioneering theories and writings of Julius Wolf and Wilhelm Roux during the late nineteenth century. Over the following decades, researchers further defined the influence of mechanical loading on bone structural adaptation. In a seminal paper by Rubin et al., it was first documented that the skeleton adapted based on the level of mechanical load to which it was exposed; removal of all external load resulted in bone loss, while just twelve minutes per day of mechanical compression increased bone mass (1). These data have served as a building block for a greater understanding of the relationship between mechanical load and bone adaptation, which now continues into its second century of study.

In addition to the interest in mechanical loading effects on skeletal tissue, there are important reasons to investigate the adaptations of bone to periods of reduced loading. This interest is motivated by the large number of individuals adversely affected by the removal of weightbearing activity through prolonged bed rest, limb immobilization after injury and spaceflight. Additionally, it is believed that some of the underlying events that lead to unloading-induced bone loss are similar to those occurring with aging, with the former simply occurring on an accelerated time frame. Therefore, research aimed at determining the mechanisms of disuse-induced bone loss will likely

---

This dissertation follows the style and format of the Journal of Bone and Mineral Research.

provide insight into age-induced bone loss, which affects millions of individuals.

Under normal weightbearing conditions, the skeleton is in a state of balance, with osteoblast-mediated bone formation coupled to osteoclast-mediated bone resorption. This results in a conservation of bone mass over time. During periods of disuse such as spaceflight, this formation/resorption balance is "uncoupled", with decreases in formation and increases (or no change) in resorption producing a loss of bone mass. Despite numerous studies confirming the decline in bone formation as a major contributor to unloading-induced bone loss, few studies have investigated the mechanisms responsible for this altered osteoblast activity. To this end, a recent review of the physiological effects of long-duration spaceflight concluded that the loss of bone mass is "one of the most serious and intractable health risks identified so far" and that "at the basic science level, little is known about the fundamental mechanisms underlying the loss of bone mineral density in microgravity" (2). These statements clearly show the need for research focused on the mechanisms of disuse-induced bone loss.

Studying spaceflight-induced bone loss is a challenging task, as few human subjects are available and non-invasive measures of bone are limited in scope. For these reasons, animal models have been developed, with the rodent hindlimb unloading model one of the best validated for the changes that occur during spaceflight (3). This model produces changes in the hindlimbs similar to those that occur in both rodents and humans during spaceflight, including loss of bone mass and decreases in bone formation. Despite the abundance of descriptive data gained from the hindlimb unloaded rodent model with respect to skeletal adaptations, data are sparse concerning the mechanisms

behind the bone formation declines. Additionally, there has yet to be a countermeasure, mechanical or pharmacological, that has preserved bone mass during continuous unloading in a mature skeleton through maintenance of bone formation, suggesting normal levels of osteoblast activity may not be possible in the absence of mechanical load.

The objective of this research was to investigate the limitations of new bone formation during mechanical unloading by superimposing the physiological stressor of marrow ablation on the skeletally mature tail suspended mouse. As marrow ablation provides a potent bone formation stimulus, these studies were designed to determine if bone formation rate increases are limited during unloading because of reduced mature osteoblast function, disrupted osteoblast proliferation/differentiation, or a combination of the two. It was hypothesized that ablation-induced bone formation would be less pronounced in unloaded animals due to both reduced mature osteoblast activity and compromised osteoblast differentiation/proliferation.

This hypothesis was tested by quantifying bone density, bone volume, percent mineralizing surface, percent osteoblast surface, mineral apposition rate and bone formation rate to assess osteoblast functionality. Additionally, osteoblast development was evaluated through quantitation of core-binding factor 1 and osteocalcin gene expression patterns, markers of early osteoblast differentiation and fully mature osteoblasts, respectively.

Specifically, the experiments detailed herein addressed the following hypotheses:

1) Unloading will reduce the bone formation response to marrow ablation by inducing deficiencies of osteoblast functionality (osteoblast surface, mineralizing surface, mineral apposition rate and bone formation rate).
2) Unloading animals for 10 days prior to ablation, so as to significantly compromise osteoblast functionality, will further reduce the ablation-induced bone formation response in unloaded bones.
3) The hypothesized attenuated osteoblast response to marrow ablation in the absence of mechanical load will be the result of a decrease in both early osteoblast differentiation and late osteoblast development. The disruption of these processes will be exacerbated if osteoblast functionality is reduced by 10 days of unloading prior to ablation.

CHAPTER II

REVIEW OF LITERATURE

To place the current study into proper context, a brief review of previous literature in the field of skeletal adaptations to unloading is necessary. This review will begin by providing background information on osteoblast development and function, the major cells of interest in this study, followed by a summary of major findings from human spaceflight/bed rest studies and animal spaceflight/ hindlimb unloading studies, with particular focus on osteoblast-related measures. Additionally, the events that take place following marrow ablation will be outlined.

Osteoblasts

Osteoblasts, the bone forming cells, originate from mesechymal stem cells (MSC) within the bone marrow and periosteum (4-6). These MSC repeatedly divide, with one of the daughter cells progressing on and the other retaining the progenitor capability (7). The hallmark of stem cells, however, is that they have non-delineated lineages, thus having the ability to transform into various cell types (5). The MSC have five known tissue lineages, which include bone, muscle, adipose, cartilage and vascular smooth muscle cells (5). It is not currently known at what point in the differentiation process commitment to a specific lineage is absolute.

Core-binding factor 1 (cbfa1; also known as Runx2) is a member of the runt homology domain transcription factor family and has been identified as the earliest known osteoblast differentiation marker (4,8). It is the only known transcription factor

specific to cells of the osteoblast lineage, its expression being restricted to post-natal osteoblast precursors called osteoprogenitors (8). The vital nature of this factor is displayed through studies of mice lacking cbfa1, which die within hours of birth as their skeleton is completely cartilaginous (8). These mice have a complete absence of both endochondral and intramembranous bone formation due to the lack of functioning osteoblasts (8). These data, along with others, document that cbfa1 plays a key role in promoting differentiation of osteoprogenitor into fully functioning osteoblasts.

Osteoprogenitor cells, present in measurable but low numbers in mouse bone marrow stroma, have two distinct populations. One of these populations appears to have the ability to constitutively differentiate, while the other inducible population only differentiates with certain stimuli (steroids or bone morphogenic proteins)(6). Although the exact mechanisms by which osteoprogenitor cells become committed pre-osteoblasts are not clear, once commitment occurs, levels of alkaline phosphatase begin to increase (9). Thereafter, pre-osteoblasts promptly proliferate, eventually becoming fully functioning osteoblasts. These cells are highly enriched in alkaline phosphatase, able to secrete type I collagen and bone matrix proteins, and express high levels of osteocalcin. Prior to the identification of cbfa1, osteocalcin was the only known osteoblast-specific gene (8). It is expressed only in post-proliferative osteoblasts which are fully mature, normally during mineralization of organic matrix (8,10).

A limited number of studies have examined changes in osteoblast cells in response to unloading, utilizing cells cultured in space or in various rotating cell culture systems (11). When cultured in space, two different osteoblast cell lines had a reduced

total cell number and altered cell morphology compared to ground control cultures (12). After one day of culture, osteoblasts had reduced mRNA expression of both early growth genes and osteocalcin, suggesting these cells are slower to enter the cell cycle in microgravity and have reduced ability to become fully functioning cells (13). When cultures were treated with 1,25D and TGF-β to stimulate rapid osteoblast development, spaceflight cultured cells had lower c-fos, alkaline phosphatase and osteocalcin mRNA (14-17). Collectivity, these reductions indicate a decrease in both differentiation and proliferation. Similarly, previous studies utilizing various forms of rotating vessels, used to effectively unload cultured osteoblasts on Earth, have documented decreases in alkaline phosphatase, collagen 1α (I), osteocalcin and cbfa1 mRNA compared to controls. Results were similar both with (18) and without stimulation with 1,25-dihydroxyvitamin D_3 (1,25-D)(19). Reductions in total cell number and an increase in apoptotic cell number have also been quantified in rotating culture experiments (20).

In summary, the pathway from mesechymal stem cell to functioning osteoblast is a complex process which is just beginning to be elucidated. A pivotal finding in advancing this process was the identification of core-binding factor 1 (cbfa1), the earliest known osteoblast-specific transcription factor and key regulator of osteoblast differentiation. Quantification of cbfa1 and osteocalcin, a marker of mature osteoblasts, provides a reliable means of studying osteoblast-specific mechanisms relevant to various skeletal-related perturbations, including disuse.

Human Disuse Studies: Bed Rest

Bed rest provides a unique Earth-based model to study the effect of microgravity on the skeleton, as it eliminates the ground reaction forces that the bones of the lower limbs normally experience during ambulation. Therefore, the only direct strain on the lower limb bones is from voluntary muscle contractions, similar to what occurs during spaceflight. As subjects for these studies are healthy volunteers, the adaptations are the result of disuse, not some underlying pathology. The majority of data on the adaptations of the human skeleton to disuse have been derived from these bed rest studies with measures of calcium balance, bone mineral content and density, serum and urine markers of bone formation/resorption, and histological measures of both cortical and cancellous bone.

The most commonly studied parameter during bed rest is calcium excretion, often reported as daily urine (and sometimes feces) output. As the skeleton is the major store of calcium in the body, increased calcium excretion without significant changes in dietary intake is usually interpreted as loss of skeletal mineral although it is important that both urine and fecal excretion be measured to determine total calcium excretion as offsetting changes could occur resulting in no net change. Increased output has been quantified after two days of bed rest (21,22), reaching levels 40% higher than baseline after one week (23). The majority of studies suggest calcium excretion peaks after 3 to 7 weeks of disuse, reaching between 21-300% higher than baseline (22,24-28) with an apparent plateau thereafter, even as far out as 9 months (25). This degree of increased

calcium excretion is substantial, ranging from 100 to 200 mg/day or 0.5 to 1.3% of total body calcium per month (22,24,25).

Changes in bone mineral content, assessed by various absorptiometry and densitometry techniques, have generally agreed with calcium excretion data. One study demonstrated that total body mineral loss (-0.08% per week) closely corresponded to total calcium excretion (-0.1% per week)(29). Regional loss of mineral content and density of the femoral neck, greater trochanter, tibia and lumbar spine range from 0.1 to 0.5% per week after 17 weeks of bed rest (27,29-31). The calcaneus, a bone of the foot that experiences the highest loads during normal ambulation, appear to be most severely affected by disuse with loss of bone mineral content averaging 1.5% per week (25,29,32).

Analysis of serum and urine biomarkers provides information regarding systemic changes in bone formation and resorption. Markers of bone formation are produced by osteoblasts as they lay down osteoid, while resorption markers are components of bone inorganic matrix that are released as during bone resorption. Urine markers of bone resorption are consistently elevated with bed rest (23,25,26,28,33-37). Significant increases have been quantified by day 4 (23) and reach levels 70 to 200% higher than baseline after 10 to 14 weeks (26,35). Osteocalcin, one of only two bone-specific proteins produced by osteoblasts, is the most commonly studied marker of bone formation. Data are inconclusive with respect to bone formation biomarkers, as studies have quantified both decreases (26,35) and no difference (23,27,33,37) in serum osteocalcin compared to baseline levels after various durations of bed rest.

Few studies have utilized histology to quantify the effects of bed rest on localized bone activity, as this requires invasive bone biopsies. After twelve-weeks of bed rest, iliac crest cancellous bone resorption surface is increased and cancellous bone osteoblast surface decreased compared to baseline measures; there is no significant change in cancellous bone volume, mineralizing surface, mineral apposition rate or bone formation rate (27). Longer duration bed rest (17 weeks) also produces no change in iliac crest cancellous bone volume compared to baseline, but trabecular number, mineral apposition rate and osteoblast surface are all reduced compared to baseline values (38,39).

In summary, data from human bed rest studies conclusively quantify rapid and substantial increases in calcium excretion, leading to decrements in bone mineral content and density. These changes in mineral and density appear to be most prevalent in cancellous bone, particularly at locations that normally experience high levels of mechanical loading. The etiology of these changes, however, is not yet well-defined due to the limited number of studies. Both whole body biomarker and iliac crest histological analyses document increases in bone resorption while some, but not all studies, demonstrate decreases in bone formation.

Human Disuse Studies: Spaceflight

Data from early bed rest studies, coupled with calcium excretion changes from the first Gemini flight, suggested that significant bone mineral loss (0.7 to 1.3% per month) would occur during spaceflight (40). Subsequent data from short term (5 to 18

day) Gemini and Apollo missions quantified bone loss of the os calcis ranging from 0-9% (41-43) accompanied by increases in urine and fecal calcium (44). As the radiographic techniques used to assess bone mineral in these studies have relatively low precision, the accuracy of conclusions based on these data has been questioned (43).

With the 1973 launch of Skylab, the first permanent inhabitable space station, followed later by Salyut-6 in 1977 and MIR in 1986, a platform for biomedical research in space was established. Increases of urinary calcium were quantified after one day of spaceflight, reaching levels 80-200% higher than preflight values after one month (41,45,46). Markers of bone resorption significantly increased after one week of flight, with levels reaching 100-200% above preflight values (36,46,47). Bone formation biomarkers were 30% lower compared to pre-flight values (47). Bone mineral content, measured pre- and post-flight using the more sensitive dual energy x-ray absorptiometry (DEXA), declined by 1 to 1.6% per month at the spine, femoral neck, trochanter, pelvis, and calcaneus; whole body mineral content loss averaged 0.3 to 0.4% per month (48). More sophisticated analyses, using computed tomography techniques, focusing on changes in cancellous bone density of the distal tibia, quantified reductions of 1.8 to 5.4% after six months of flight (49,50).

In summary, relatively few studies have assessed skeletal adaptations to spaceflight in humans. This makes global conclusions difficult, although it is clear that, similar to bed rest, bone mineral loss occurs rapidly and is significant in magnitude. The result of this mineral loss is reduced bone density, with the cancellous bone compartment of weightbearing bones most severely affected. The etiology for these

changes is not clear, with even fewer data than bed rest studies. Changes in biomarkers of bone formation and resorption mimic those from bed rest with no histological data published to date.

Animal Disuse Studies: Spaceflight

Although studies on human adaptations in space provide the most useful data, limitations with respect to subject numbers and types of studies that can be performed in-flight make conclusions difficult to draw. Thus, most of what we have learned about spaceflight-induced adaptations is derived from animal studies of both primates and rodents, with the former providing data that are more applicable to humans, although they are almost as rare.

Non-human primate spaceflight studies, while only short-term (9 to 14 days) and with few subjects (1 to 2 per mission), provide valuable data due to the invasive measures that are possible. Decreases in bone mineral density range from -1.7 to -17% depending on the anatomical site (51,52) in skeletally mature animals. One additional study concluded that space flown monkeys failed to gain bone density as measured in ground controls, likely a function of studying younger animals still accruing bone mass (53).

Iliac crest cancellous bone volume of space flown monkeys is significantly lower than that in ground controls, accounted for by decreases in trabecular thickness with no change in trabecular number (52,54). Additionally, osteoblast surface, osteoid thickness, mineralizing surface, mineral apposition rate and bone formation rate in iliac cancellous

bone are all significantly lower compared to controls (52,54). Serum measures of alkaline phosphatase (55) and osteocalcin (56), markers of osteoblast activity, are also lower compared to control values. Additionally, in vitro studies of marrow cells taken from flight monkeys reveal decreased mineralization (52,56), osteoblast proliferation (54,56) and osteoblast differentiation (57).

The most abundant spaceflight animal data is derived from rodents, particularly rats. It is important to note, however, that nearly all rodent studies during spaceflight have utilized relatively young (less than three-month-old) animals, making interpretation difficult as a large part of the unloading effect is an attenuation of growth. This growth attenuation is manifested in bone through alterations of modeling, rather than alterations of remodeling, as would occur in skeletally mature bone.

The earliest rodent spaceflight study, a 22-day mission aboard Cosmos-605, used light and electron microscopy to qualitatively document significant metaphyseal bone loss compared to controls (58). Subsequent quantitative studies have confirmed these observations, documenting lower cancellous bone volume of the proximal tibia (59-62), humerus (60,63), vertebrae (62) and pelvic bone (64) in space flown rats compared to ground controls. Some studies, however, have found no changes with unloading in bone volume of the vertebrae (63,65), humerus (65,66) and femur (61,62) compared to controls. In those studies that did quantify altered bone volume, both trabecular thinning (61,64) and lower trabecular number (59,63) accounted for the reductions.

Despite the apparent discrepancy of changes in bone volume, osteoblast-related parameters are consistently reduced in skeletally immature rats during spaceflight.

Cancellous bone osteoblast surface is reduced, compared to ground-based controls, in the tibia (60-62), vertebrae (62,63,65), femur (62), humeri (63,66) and pelvis (64). Interestingly, decreases in osteoblast surface are also observed in the mandible, a non-weightbearing bone, suggesting that spaceflight may have effects on osteoblast cells independent of changes in mechanical load (67). Accompanying these changes in osteoblast bone surface are decreases in mineral apposition rate and bone formation rate (64,66), indicating reduced functional capacity of those osteoblasts which still existed and/or reduced number of active surfaces. Gene expression data support these findings as both osteocalcin and type I collagen mRNA expression are reduced in metaphyseal bone post-flight compared to ground controls (68,69). Indices of resorption, osteoclast number and/or eroded surfaces are not significantly different from ground controls at metaphyseal bone sites (60,62,66).

In summary, primate and rodent spaceflight data document reductions of cancellous bone volume at multiple sites. Serum biomarkers, cancellous bone histology, gene expression and marrow cell culture data have all quantified significant decreases in various osteoblast parameters (number, activity, proliferation and differentiation). To date, no studies have documented changes in osteoclast histological parameters. It is important to note, however, that most published data are based on immature skeletons and do not necessarily reflect adaptations that may occur in mature skeletons.

Animal Disuse Studies: Hindlimb Unloading Model

During the mid-1970s, in the midst of the Cosmos space missions, the need for an Earth-based model to simulate microgravity in animals became clear as the number of animals that could be flown on missions was (and remains) very limited. The criteria for an acceptable model were five-fold: allow ambulation using only the forelimbs; unload the hindlimbs without paralysis or rigid immobilization; produce cephalic fluid shifts; allow normal eating, drinking, and grooming; and produce minimal stress. The tail suspended rat model as developed by Emily Morey-Holton met all necessary criteria (70). Early 20-day experiments in young rats resulted in significant reductions in tibial cortical bone formation similar to those observed after 20 days of spaceflight on Cosmos missions suggesting it was an acceptable model for studying skeletal adaptations to unloading (70). Since this early study, the model has taken many forms, both in name (simulated weightlessness, tail suspension, hindlimb unloading, etc.) and details of the harnessing system design. By late 2002, it had become the standard rodent model to study adaptations to microgravity, with over 800 publications covering numerous physiological systems (3).

When assessing the rodent hindlimb unloading literature, there is unfortunately little standardization among studies in regard to animal age, duration of unloading, site of analysis and the type of assessment. Despite these differences, some generalizations can still be made from the data. An overwhelming number of studies utilized one- to three-month-old animals, an age of rapid bone growth, and maintain unloading for 3 to 24 days, depending on the outcome measure of interest. The most common skeletal sites

studied in young rats have been the proximal and mid-diaphyseal tibia, proximal, mid-diaphyseal, and distal femur and vertebrae. Early studies used relatively simple analyses, such as measures of whole bone mass, while recent studies have progressed to utilize micro-computed tomography (microCT) and gene expression analyses. Histomorphometry, however, has remained the gold standard, providing the most data over the years with regard to cellular adaptations to unloading.

Whole tibial bone mass is significantly lower than weightbearing controls after 7 to 14 days of unloading (71-73). Beyond this time period, however, bone mass accrual occurs at rates similar to control animals, suggesting simply an acute attenuation of growth during unloading, with an eventual return to normal rates (71). Changes in calcium content mimic those of total bone mass, with decrements in tibia and vertebrae calcium content observed at both 7 and 14 days (71,74,75). Regional changes, however, differ from whole bone measures, with proximal tibia continuing to lose bone density over three weeks (76). Changes in skeletal calcium uptake and matrix accretion, assumed to reflect osteoblast activity, mimic those of bone mass as they are significantly reduced after 5 days of unloading and return to control values by days 10 to 15 (71,74).

Proximal tibia cancellous bone volume is similar to weightbearing controls after 4 to 5 days of unloading (77,78). Significant reductions are detectable by day 6 (79) with a continued depression compared to controls through day 14 (72,75,76,80). This lower bone volume is accounted for by decreased trabecular thickness (72,75,79) and trabecular number (75). Mineral apposition and formation rates of proximal tibia cancellous bone are lower compared to controls after 4 to 8 days (73,76-78, 80),

although mineral apposition rate returns to control levels around day 14 (75,76,80). Measures of osteoblast and osteoid bone surface are reduced compared to controls after just 4 days of unloading (77) and remain lower through 14 days (73,75,78,79,81). Measures of resorption such as osteoclast/eroded bone surface are not different in unloaded cancellous bone compared to controls (75,76,79,80).

Short-term studies, designed to assess changes of gene expression, consistently document reductions of osteoblast markers. After five days of unloading, osteocalcin mRNA is significantly reduced (68) while by day 7 to 8, Cbfa1, osteocalcin and collagen Iα mRNA expressions are at non-detectible levels (77). Alkaline phosphatase mRNA expression also progressively decreases through 14 days of unloading (68). Collectively, these data suggest a retardation of osteoblast maturation with unloading.

A limited number of studies have also examined cellular composition of bone tissues after unloading, with data suggesting reductions in osteoblast progenitor cells. After 6 days of unloading, both proximal tibia metaphysis and marrow cavity reveal 80% fewer preosteoblasts compared to controls (79). Detailed study of proximal tibia primary spongiosa, a highly cellular portion of the bone rarely studied due to its lack of mineralized tissue, documented a reduction in differentiated osteoprogenitor cells and fewer pre-osteoblasts (82). These data suggest a reduced differentiation and proliferative capacity of osteoprogenitor cells during unloading.

Cell cultures of marrow harvested from unloaded rats provide additional data with regard to changes in cell development/function. Following 2 to 5 days of unloading, cell culture mineralization is reduced coupled with a reduction in overall cell

proliferation, alkaline phosphatase and c-fos mRNA production (83). Longer periods of unloading yield similar results: reduced expression of osteocalcin (83) and alkaline phosphatase (78, 84), mineralizing colonies (78), and total number of cells (84) as compared to those in control rat marrow cultures.

While the above data provide pivotal information with regard to changes in the unloaded skeleton, the use of animals that are still undergoing rapid bone growth make interpretation difficult. Do reduced bone density and volume compared to ground controls really reflect bone loss, or simply a lack of bone gain during growth? This question is substantiated by the finding that bone mass accrual in young unloaded rats proceeds at similar rates as controls after 7 to 14 days of unloading, and mineral apposition rate returns to control levels during a similar time frame. Therefore, it is useful to eliminate the effects of growth by studying skeletally mature animals during unloading. Although the rat continues to slowly increase body mass throughout its life, the rate of skeletal growth slows significantly after 5 months of age (85). More recently published studies have used skeletally mature rats and reveal distinct differences compared to young, growing rats.

Five-month-old rats exhibit reduced proximal tibia cancellous osteoblast surface (86) despite no change in bone volume after just one week of unloading; by day 14, tibial mineral content and density are significantly lower than controls (87). Unloading for longer durations, 28 to 40 days, results in significant reductions in cancellous bone volume (80) and bone density (88). Additionally, mineral apposition rate, mineralized surface and osteoblast surface are reduced compared to weightbearing controls with no

difference in osteoclast surface (86,89). These prolonged decrements in bone formation (through 35 days) are in direct contrast to the transient (7- to 14-day) reductions quantified in skeletally immature animals.

Hindlimb unloading studies have also been carried out using mice, a species that provides certain advantages over the rat model, such as the potential to use genetically modified strains (90,91). Interpretation of mouse data, however, must be carefully considered, as there is a significant effect of genetic background on the skeleton (92). Studies of 12-month-old female mice from multiple genetic strains reveal that the C3H/HeJ (C3H) strain has a 50% higher total femoral density compared to the C57BL/6J (B6) mouse, which has the lowest density of those strains examined (92). Additional analyses of these two strains quantified differences in distal femur cancellous bone volume at four months (93) yet cancellous osteoid surface, mineral apposition rate and bone formation rate were similar (93).

The most common genetic background used in bone-related hindlimb unloading studies is the B6, "low-density" mouse (94-100), although data do exist from the C3H, "high-density" mouse. Following 21 days of unloading, four-month-old female C3H mice exhibit non-significantly lower proximal tibia bone volume, mineral apposition rate and bone formation rate (-31, -6 and -39%, respectively) compared to baseline controls (100). Similar age C3H male mice, suspended for 14 to 21 days, exhibited no change in bone volume or mineral apposition rate compared to control (97), suggesting a within-strain gender difference in the bone response to unloading.

In summary, data from hindlimb unloaded rodent models reveal changes similar to those observed in space flown rodents. Cancellous bone is most severely affected due to significant decrements in osteoblast development and function, whereas resorption parameters are not significantly different. Skeletally mature animals have been studied during ground-based hindlimb unloading, and have generally confirmed decreases in cancellous bone volume and density, osteoblast surface and bone formation rate with no change in osteoclast parameters. One fundamental age-dependent difference, however, is that young animals have only transiently lower mineral apposition rate, bone formation rate and bone mass accrual, while skeletally mature animals have continued depression of these values through 35 days of mechanical unloading.

Marrow Ablation as a Bone Formation Stimulus

Since the 1960's, research concerning long bone marrow regeneration has been undertaken, often as it relates to local tissue injury. Early studies provided much of what is currently known regarding the series of events that follow removal or disruption of marrow from long bones (101,102). These early studies speculated that the disruption of the continuum of marrow stroma initiated these processes, as disruption without removal (ablation) of marrow produced similar results. Subsequent research in both rats and mice has helped define the sequence of events that follow marrow ablation, with no notable differences identified between the two species (for summary of key ablation related skeletal events see **Figure 1**).

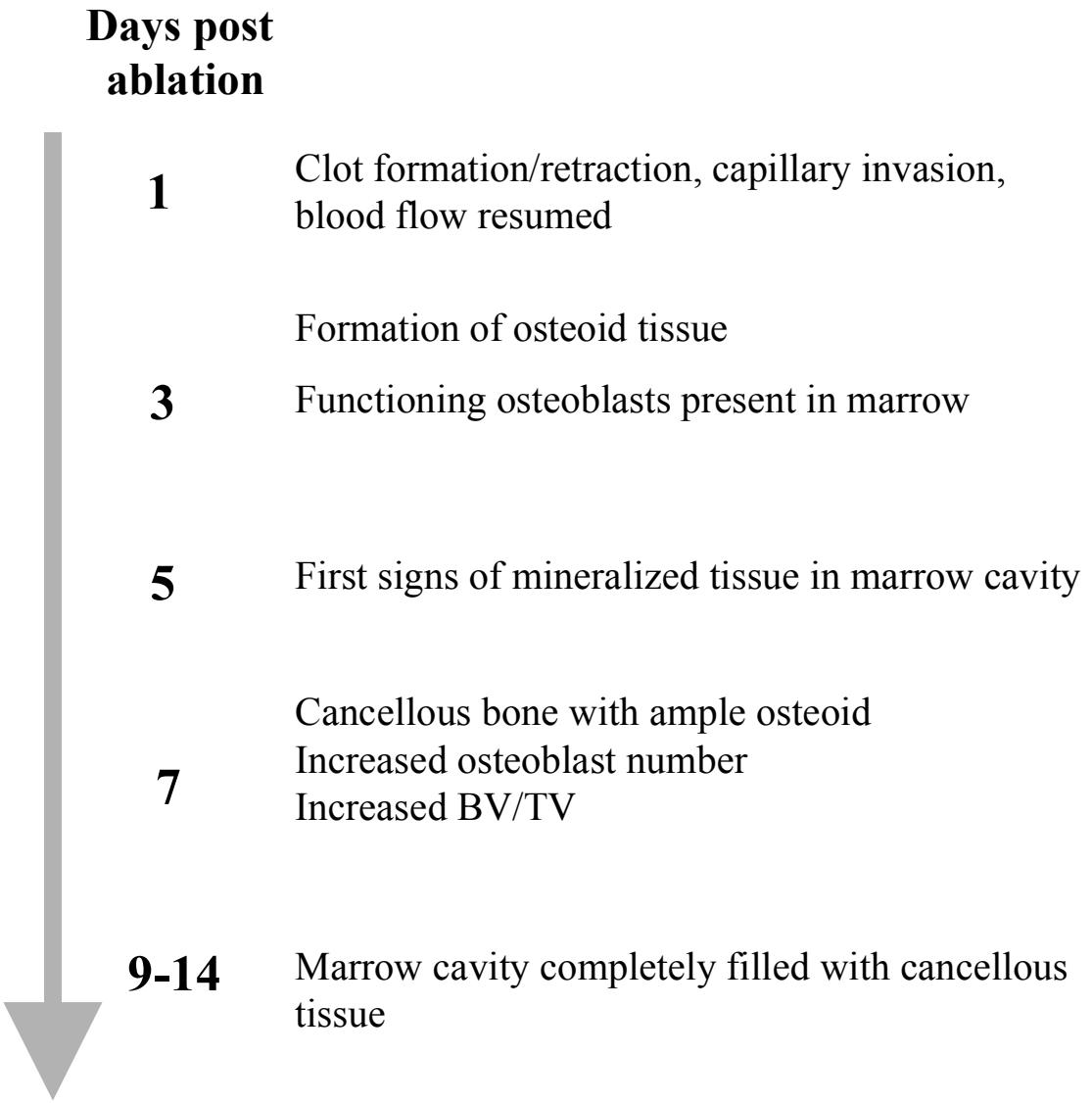

FIG. 1. Timeline of significant events during the "osteogenic period" following marrow ablation. These results are derived from both rat and mouse studies (103-106,108).

Immediately following marrow ablation, a blood clot fills the marrow cavity and then retracts soon afterward, allowing reformation of the marrow cavity blood vessel network (103). This allows resumption of blood flow, providing a means through which cells (thought to be pre-osteoblasts) from the surrounding cortical bone can migrate to the marrow cavity. These cells, along with stromal cells remaining after ablation (e.g. attached to endocortical surface, among trabeculae), play the largest role in marrow regeneration. It is important to note that these stromal cells have little migratory potential, with no evidence of movement from the epiphyses to other under-populated areas (102). By day 3, a rudimentary trabecular network with faint signs of mineralization has formed (103) and osteoblasts begin proliferating and forming osteoid. Osteoblast-lined trabecular bone, growing out from the endocortical surface, is observed by 6 days post-ablation, increasing in volume by day 8 (103). By this time, mineral apposition rate, osteoid volume and osteoblast surface have increased substantially compared to untreated controls (104). Bone formation rate and bone volume peak between days 6 and 14 (103,105,106). There is no significant change in bone resorption parameters refuting an increased turnover argument (104,107). This "trabecularization" of the marrow cavity is vital, as without it neither increased bone formation nor marrow regeneration occur. Soon after this peak bone volume is attained, marrow sinusoids develop, allowing marrow cells to repopulate the cavity. Increases in osteoclast number then occur, which eventually resorb the majority of the newly formed cancellous bone. Full marrow regeneration is complete by 20 to 30 days after ablation, with all surfaces

having osteoblast-related parameter values (bone volume and formation rate) comparable to non-ablated controls (103).

Molecular biology studies have provided insight into the mechanisms of these responses to marrow ablation. By day 5 after ablation, alkaline phosphatase mRNA is significantly elevated four-to-five fold (103,105,108); osteocalcin expression is similarly elevated by day 6 (103,105,106). In situ hybridization (109) and in vivo real-time bioluminescence (110) have also quantified significant increases in osteocalcin mRNA within the first week post-ablation. Levels of pro-collagen α (I) mRNA reached maximum levels by day 6 (103,105), with α (II) and α (III) levels unchanged (103). As levels of pro-collagen α (II) mRNA expression often increase in response to fracture injury, this suggests the deposition of bone following ablation is different from callus formation after fracture, another example of rapid bone formation (105). The early rise in alkaline phosphate and pro-collagen α (I) mRNA expression reflect increases in preosteoblasts and proliferating osteoblasts, while later increases in osteocalcin mRNA suggests increased numbers or activity of mature osteoblasts (105).

In summary, marrow ablation results in a well-defined series of events highlighted by a significant increase in osteoblast and bone formation parameters 7 to 14 days post-ablation (**Figure 1**). These parameters have been quantified by numerous methods including histology, densitometry and gene expression. While the majority of marrow ablation studies have utilized rats, the few that have quantified responses in mice reveal no differences with respect to temporal and qualitative events. Although the specific mechanism of marrow trabecularization in response to ablation are not known,

most data suggest that local stromal cells remaining on trabeculae and endocortical surfaces, along with pre-osteoblasts arriving through the circulation, play a significant role through differentiation and proliferation into osteoblasts.

CHAPTER III

RESEARCH

During prolonged periods of non-weightbearing activity, such as bed rest, immobilization and spaceflight, weightbearing bones experience significant loss of bone mineral (1 to 2% per month) (29,49,50). Human serum and urine biomarker data suggest that changes in both bone formation and resorption contribute to disuse-induced bone loss, as bone resorption markers are consistently increased (26,35,36,46,47) and bone formation markers are consistently decreased (26,35,47). Histology data on bone biopsies from bed rest subjects, which directly assess localized tissue level changes at the iliac crest, suggest that bone formation changes to a greater degree than does resorption. Significant decreases in osteoblast surface (27,38,39) and mineral apposition rate (38,39) in these subjects are accompanied by minimal changes in osteoclast surface (27).

Due to the limitations of studying disuse-induced changes in humans, particularly during spaceflight, the rodent hindlimb unloading (HU) model was developed. This model has been used extensively to study physiological adaptations of many tissues to spaceflight, including the skeleton (3,70). In skeletally immature rats (1- to 3-months-old), hindlimb unloading produces significant depressions in cancellous bone formation rate and increases in bone resorption. However, these changes return to control levels after 14 days, suggesting only transient perturbations of bone turnover in unloaded, growing animals (71,74). Studies on skeletally mature rats ($\geq$ 5 months old) have also documented significant decrements in cancellous bone mineral density, mineralizing

surface, osteoblast surface and bone formation rate with unloading; however, these changes persist through 28-35 days of unloading (86,88). Additionally, there is no change in cancellous bone osteoclast/eroded surfaces (86). Unloading-induced reductions in cancellous bone volume (97,100,111) and bone formation rate (97,100,111) have also been documented in skeletally mature mice after 14 to 28 days.

Few studies to date have investigated the underlying mechanisms responsible for decreased osteoblast activity during disuse. Cultures of marrow from unloaded long bone (78,83) and of osteoblasts grown in unloaded environments (13,19) suggest decrements in proliferation and differentiation. Another indirect method used to elucidate mechanisms is through application of various countermeasures. Both mechanical and pharmacological interventions have had variable success with respect to bone parameters (mass/density), yet no study to date has documented maintenance of bone formation rate in continuously unloaded skeletally mature animals. It is therefore unclear whether disuse-induced declines in osteoblast functionality can be attenuated in a mature skeleton.

Marrow ablation (removal of the marrow from a long bone) results in a rapid formation of cancellous bone throughout the entire marrow cavity (103). Once this cancellous scaffolding has been provided, marrow regeneration proceeds, after which the bone scaffold is resorbed. This experimental model is unique in that the cancellous bone formation follows a well-defined series of events, highlighted by a significant increase in bone formation parameters including osteoblast surface and bone formation rate. Within days of ablation, localized osteocalcin gene expression (103,106,108) and bone

formation rate (104,106) are significantly increased while by day 7 to 14 cancellous bone has filled a majority of the marrow cavity. Due to the potent and rapid osteoblast-stimulating effect of marrow ablation, it may serve as an excellent model with which to study the effects of hindlimb unloading on osteoblast differentiation, proliferation and function.

Therefore, the research described herein was designed to investigate the limitations of bone formation during unloading by superimposing the physiological stressor of marrow ablation on the hindlimb unloaded mouse. Specifically, the following hypotheses were tested: 1) ablation-induced increases in osteoblast functionality will be reduced in unloaded mice compared to weightbearing controls, 2) unloading for 10 days prior to ablation, so as to compromise osteoblast functionality, will further reduce the osteoblast response to marrow ablation in unloaded bone, 3) the reduced osteoblast response to ablation in unloaded bone will be the result of a decrease in both differentiation and proliferation. Key outcome measures used to address these hypotheses included static and dynamic cancellous bone histomorphometry, bone densitometry by peripheral quantitative computed tomography (pQCT), and real-time PCR analyses of gene expression.

Methods

The following study protocols and all animal procedures were in compliance with the Texas A&M University Laboratory Animal Care Committee rules and regulations.

Study one. Four-month old C3H/HeJ (C3H) male mice from Harlan (Indianapolis, IN) were housed individually in a temperature-controlled room (21 ± 2°C) with a 12:12 hour light/dark cycle and provided free access to standard chow and water throughout the experiment. Preliminary studies revealed a significant increase in bone volume in response to ablation in this age/strain mouse. One week after arrival, mice were randomly assigned into treatment groups (n=6-8 per group): baseline control (BC), cage control + marrow ablation (CCAB), hindlimb unloaded (HU), and hindlimb unloaded + marrow ablation (see **Table 1** for experimental outline). The hindlimb unloaded + marrow ablation animals were further divided into two groups (n=6-8 per group) which differed by when marrow ablation was performed. One group underwent ablation on the day of unloading (HUAB) while the other was unloaded for 10 days prior to ablation (HU10AB). Groups of animals were sacrificed at two separate time points, 10 and 14 days post-ablation, both falling within the osteogenic period (**Figure 1**)(103,104,106), in the event that unloading delayed bone formation responses.

On day 0, all animals were anesthetized (0.33mg/kg fentanyl citrate, 16.7 mg/kg droperidol, and 5.0 mg/kg diazepam) and underwent right femur marrow ablation and/or hindlimb unloading. When ablations were performed on animals after 10 days of unloading, animals were completely anesthetized before removal from suspension to avoid any weightbearing by the hindlimbs. On day 4 and 2 prior to sacrifice, animals were injected intraperitoneally with calcein (20 mg/kg) to allow for dynamic histological measurements. On day of sacrifice, animals were euthanized using sodium pentobarbital (200 mg/kg, IP). The distal 2/3 of the right femora were removed, placed in 10%

TABLE 1. STUDY ONE DESIGN

	Days				
	0	10	14	20	24
BC	X				
CCAB	AB	X	X		
HU	HU	X	X	X	X
HUAB	AB+HU	X	X		
HU10AB	HU	AB		X	X

CCAB, cage control + marrow ablated. HU, hindlimb unloaded; HUAB, hindlimb unloaded + marrow ablation on day 0; HU10AB, hindlimb unloading + marrow ablation on day 10; AB, marrow ablation. X denotes group of n = 6-8 animals sacrificed at that time point.

formalin for 24 hours, and then transferred to 70% ethanol for peripheral quantitative computed tomography (pQCT) and histological analyses.

Study two. In order to assess the effect of ablation on markers of osteoblast differentiation and proliferation, procedures similar to study one were performed with groups sacrificed at earlier time points for gene expression analyses. All animal procedures were similar to study one except that no calcein injections were performed. Groups (n=6/gp) of CCAB, HUAB and HU10AB animals were sacrificed at 1, 3 and 10 days post-ablation (see **Table 2** for experimental outline). Baseline controls (BC) were sacrificed on day 0 as a comparison group. These time points were chosen, based on previous studies (103,106,108), to assess early and late changes in osteoblast-related gene expression. At sacrifice, the distal 2/3 of right femora were excised, snap frozen in liquid nitrogen, and stored at –80◦C for polymerase chain reaction (PCR) analysis.

Hindlimb unloading. Unloading of the hindlimbs was achieved by tail suspension with minor modifications (3). Briefly, a wire harness was applied to middle 2/3 of the tail using cyanoacrylate. The tail harness was attached to a metal swivel and then connected to a support that spanned the housing cage (5 x 7 x 12”). The height of the animal’s hindlimbs was adjusted to prevent any contact with the cage bottom, resulting in approximately a 35 to 40º head-down tilt. The mouse was able to access about 80% of the cage, with traction provided by a wire mesh which covered the cage bottom.

Marrow ablation. Animals in select groups underwent right femoral marrow ablation as previously described with slight modifications (103,112). Once the mouse was anesthetized, hair was removed from the right hindlimb. Using aseptic techniques, a 1-

TABLE 2. STUDY TWO DESIGN

	Days						
	0	1	3	10	11	13	20
BC	X						
CCAB	AB	X	X	X			
HU	HU	X	X	X	X	X	X
HUAB	AB+HU	X	X	X			
HU10AB	HU			AB	X	X	X

CCAB, cage control + marrow ablated. HU, hindlimb unloaded; HUAB, hindlimb unloaded + marrow ablation on day 0; HU10AB, hindlimb unloading + marrow ablation on day 10; AB, marrow ablation. X denotes group of n = 4-6 animals sacrificed at that time point.

inch incision through the skin was made on the anterior leg across the knee joint and, using the distal femoral condyles as a landmark, a 25 gauge needle was inserted into the mid-condylar notch. The needle was removed and a 25 gauge dental drill inserted into the same hole, rotated clockwise/counterclockwise several times, and then removed. A 27 gauge needle attached to a 3 mL syringe filled with 1.5 mL sterile water was inserted and the marrow cavity back-flushed, extruding the marrow. The needle was removed and the open skin wound cleansed using sterile gauze-tipped swabs. The incision was closed using cyanoacrylate and betadyne applied to prevent infection. Upon recovery, animals had full ambulatory capacity. Animals in HU + ablation groups were unloaded as soon as they had recovered from the anesthesia, with an attempt to minimize any weightbearing before unloading began.

Peripheral quantitative computed tomography (pQCT). *Ex vivo* scans of the right femora were performed using a XCT Research M (Stratec; Norland Corp., Fort Atkinson, WI). This model has a minimum voxel size of 0.07 mm and a scanning beam thickness of 0.50 mm and has previously been used successfully to detect differences in mouse femora density following marrow ablation (112). Two slices, located at 3 and 4 mm proximal to the distal condyle plateau, were scanned at a resolution of 0.07 x 0.07 x 0.50 mm. This location was selected to match that of histological assessment of metaphyseal bone. Each of the two slices was analyzed for cancellous bone mineral content (BMC) and density (BMD), as well as total and marrow area, with the data averaged to get a single value for each bone metaphyseal region. Total area is defined as all area encompassed by the periosteal surface while marrow area is the area within the

endocortical surface. Coefficients of variation for measures of cancellous BMC, BMD, total area and marrow area, based on five repeat scans of the same bone with repositioning between scans, were ± 2.2, 3.1, 1.7 and 1.3%, respectively.

Histomorphometry. Following pQCT, undemineralized right femora were subjected to dehydration using graded ethanols followed by xylene, and finally embedded in methylmethacrylate. Serial longitudinal sections (4 μm) were cut using a motorized rotary microtome (HM355, Carl Zeiss; Thornwood, NY) and affixed to slides. For each bone, one slide was left unstained for fluorochrome label measurements while another was processed with the Von Kossa staining procedure for cellular measures. All histological analyses were performed using BioQuant TrueColor Windows image processing analysis system (R&M Biometrics, BQTCW98, Version 3.50.6) interfaced with a light microscope (Olympus, Leeds Instruments, Irving, TX).

Dynamic histomorphometry data were collected on unstained sections under epifluorescent light. Briefly, a 1.5-2 mm^2 region of interest, located approximately 0.5 mm distal to the growth plate, was defined at 40x magnification. Within the defined area, single (sLS) and double (dLS) labeled surfaces were measured at 100x while inter-label widths were measured at 200x. Calculated variables based on raw data measures included: mineral apposition rate (MAR, μm/d), calculated by dividing the inter-label width by the time between labels (2 days); percent mineralizing surface (MS/BS, %), calculated using the formula [((sLS/2) + dLS)/total bone surface]*100; and bone formation rate (BFR, mcm^3/mcm^2/day), calculated as (MAR * MS/BS). All measures and variables conform to recommended bone histomorphometry standards (113).

Static cell surface histomorphometry data were collected on stained sections with the region of study similar to that of dynamic analyses. Bone volume (BV/TV, %) and bone surface (BS) were assessed at 40x magnification while osteoblast and osteoid surface, measured at 200x magnification, were combined and presented as a percent of total bone surface (Ob.S). Osteoblasts were defined as single nuclei cuboidal cells lining a cancellous bone surface while osteoid was identified by its light blue staining pattern.

Real-time PCR. Femora, stored at –80°C, were homogenized using a freezer mill (SPEX CertiPrep, Inc, Metuchen, NJ) and total RNA isolated using RNA-STAT 60 (Tel-Test, Inc., Friendswood, TX), according to the manufacturer's protocol. Levels of steady state mRNA for osteocalcin (OC) and core binding factor 1 (cbfa1) were determined by quantitative real-time RT-PCR. Denatured total RNA from the bone samples (1 μg) was reverse-transcribed to cDNA using TaqMan Reverse Transcription Reagent (Applied Biosystems, Foster City, CA) in a 20μL reaction. Oligonucleotide primers and TaqMan probes for PCR amplification were designed (**Table 3**) based on murine sequences using Primer Express software (Version 1.0) and synthesized with a FAM reporter fluorescent dye using Assay-by-Design service (Applied Biosystems, Foster City, CA). After reverse transcription, 2μL cDNA was amplified and quantified using the ABI PRISM 7700 Sequence Detection System (Applied Biosystems, Foster City, CA) according to manufacturer's protocol. All samples were performed in duplicate with expression levels normalized to 18S RNA from the same sample, simultaneously amplified under similar conditions (30 min at 48°C, 10 min at 95°C, 40 cycles of 15 sec at 95°C and 1 min at 60°C). Fluorescence data collected during PCR

TABLE 3: OLIGONUCLEOTIDE PRIMERS AND TAQMAN PROBES FOR CDNA PCR AMPLIFICATION

Oligonucleotide	Sequence (5' to 3')
Cbfa1 TaqMan probe	CCATCTTTGGGAAACTA
Cbfa1 forward primer	GCTGCGCTCTGTCTCTCTGA
Cbfa1 reverse primer	TGAGACCTTCAGGAGGGTAGTTACC
OC TaqMan probe	CCGGGTTCATTTCT
OC forward primer	TCCAAGAGGGCAAAAGAAGAGA
OC reverse primer	CGTCTTGATTTGCTAATTCTGATTCA
18S TaqMan probe	
18S forward primer	Applied Biosystems, Part No, 4308329
18S reverse primer	

Cbfa1, core binding factor 1; OC, osteocalcin

were analyzed using ABI-Prism software and reported as expression relative to baseline control levels, as previously described (114).

Statistical analyses. All statistical analyses were performed using SAS software (Version 6.12). Percent change in body mass was assessed using two-way analysis of variance (ANOVA) on data combined from both studies. Skeletal parameters from study one were evaluated using specific group comparisons determined *a priori* to assess 1) the effect of unloading, 2) the effect of ablation in unloaded compared to weightbearing controls and 3) the effect of ablation timing on the response in unloaded animals. The independent effect of unloading was assessed by one-way ANOVA using baseline control and the four HU groups, with significant main effects tested for group differences using Duncan post-hoc analyses. The effect of ablation in unloaded vs. weightbearing controls was assessed with three-way ANOVA on load (CC or HU), treatment (ablation or non-ablation) and time (10 or 14 days) using right (ablated) leg values from baseline controls, CCAB, HU and HUAB groups. As no significant interaction existed between time and treatment/load for any parameter, data were pooled across days and two-way ANOVA analyses were performed to define load and treatment effects, with Duncan post-hoc tests used if significant interactions existed. To assess the effect of ablation timing in unloaded animals, ablated limbs of HUAB, HU10AB and time-matched HU non-ablated controls were pooled across post-ablation day (10 and 14) and assessed using a two-way ANOVA of treatment (ablation or non-ablation) and day of ablation (0 or 10 days HU). Relative expression levels of mRNA from study two were analyzed by two-way ANOVA on treatment (HU, CCAB and HUAB) and time (1,

3 and 10) using Bonferroni post-hoc tests. Statistical power for all reported analyses was ~ 0.80 unless otherwise noted. All values are reported as mean ± SE and a p value < 0.05 was used to determine statistical significance, while differences of $p < 0.10$ are noted in the text as trends.

Results

Body mass effects of unloading: All groups had similar body masses at baseline. There was no difference between HUAB and HU10AB body mass changes compared to HU at any time point, thus all HU animals were pooled within time across studies one and two (data not shown). There was a significant difference, albeit minimal (< 3%) in percent body mass change from baseline compared to time-matched controls at all time points through day 14 (**Figure 2**).

Skeletal effects of unloading. Hindlimb unloading did not result in significant changes in distal femoral metaphysis cancellous bone mineral content (BMC) or density (BMD) at any time point up to 24 days (**Table 4**). Cancellous bone volume (BV/TV) and percent osteoblast/osteoid surface (Ob.S) were both significantly lower than baseline controls by day 14 (-31 and -45%, respectively) remaining lower through day 24. There was no significant effect of unloading on marrow area, percent mineralizing surface (MS/BS), mineral apposition rate (MAR) or bone formation rate (BFR).

Unloading effects on ablation-induced bone formation. Marrow ablation resulted in significantly higher cancellous BMD in both control and unloaded animals (CCAB: 472 ± 6; HUAB: 456 ± 15 mg/cm^3) compared to non-ablated controls (BC: 280 ± 8; HU: 262 ± 10 mg/cm^3) (**Figure 3A-B and 4A**). There was no difference between the ablated

TABLE 4. EFFECTS OF UNLOADING ON DISTAL FEMUR SKELETAL PARAMETERS

	Days of hindlimb unloading				
	0	10	14	20	24
BMC, mg/mm	0.29 ± 0.03	0.24 ± 0.01	0.24 ± 0.02	0.27 ± 0.03	0.27 ± 0.02
BMD, mg/cm^3	280 ± 19	276 ± 8	275 ± 20	268 ± 16	256 ± 13
Marrow area, mm^2	0.99 ± 0.09	0.86 ± 0.04	0.89 ± 0.07	0.96 ± 0.06	1.03 ± 0.08
BV/TV, %	10.9 ± 1.0	8.6 ± 1.0	7.5 ± 1.1 *	6.0 ± 0.57 *	7.3 ± 1.1 *
Ob. S, %	3.1 ± 0.7	1.7 ± 0.7	1.6 ± 0.2 *	1.7 ± 0.3	1.5 ± 0.4 *
MS/BS, %	25 ± 4	18 ± 4	17 ± 8	22 ± 4	24 ± 4
MAR, μm/day	2.1 ± 0.1	1.7 ± 0.2	1.6 ± 0.5	1.9 ± 0.1	1.8 ± 0.1
BFR, μm^3/μm^2/day	55 ± 11	34 ± 10	36 ± 18	47 ± 10	47 ± 8

Distal femoral metaphysis parameters assessed by peripheral quantitative computed tomography (BMC, BMD, % marrow area) and histology (all others). Data are mean ± SE with n = 6-8 per group. BMC, bone mineral content; BMD, bone mineral density; BV/TV, bone volume per tissue volume; Ob.S, osteoblast surface expressed as percent of total bone surface; MS/BS, mineralizing surface per total bone surface; MAR, mineral apposition rate; BFR, bone formation rate. Marrow area denotes area within the endocortical surface. All data refer to cancellous bone. * denotes significant difference vs. baseline controls (0-d HU) ($p < 0.05$).

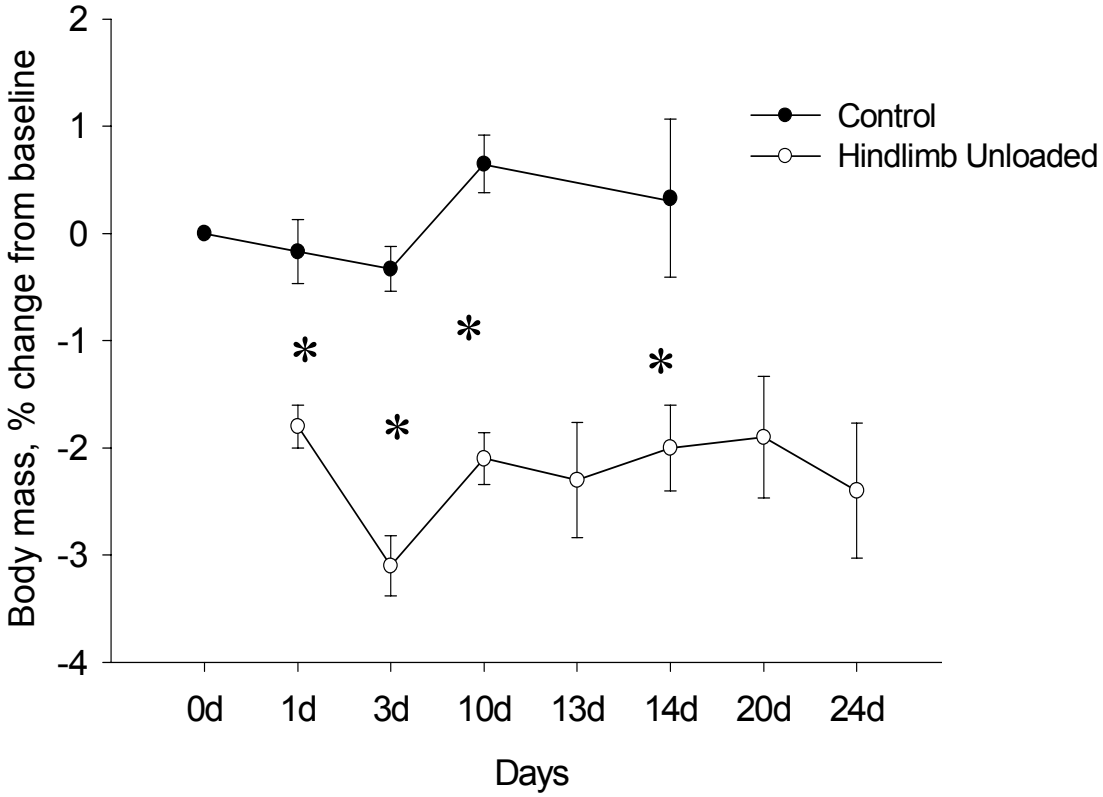

FIG. 2. Effect of unloading on body mass changes of skeletally mature C3H mice. Hindlimb unloaded data are pooled from both non-ablated and ablated animals as there was no significant effect of ablation on body mass changes. * denotes significant difference ($p < 0.05$) vs. time-matched cage control animals.

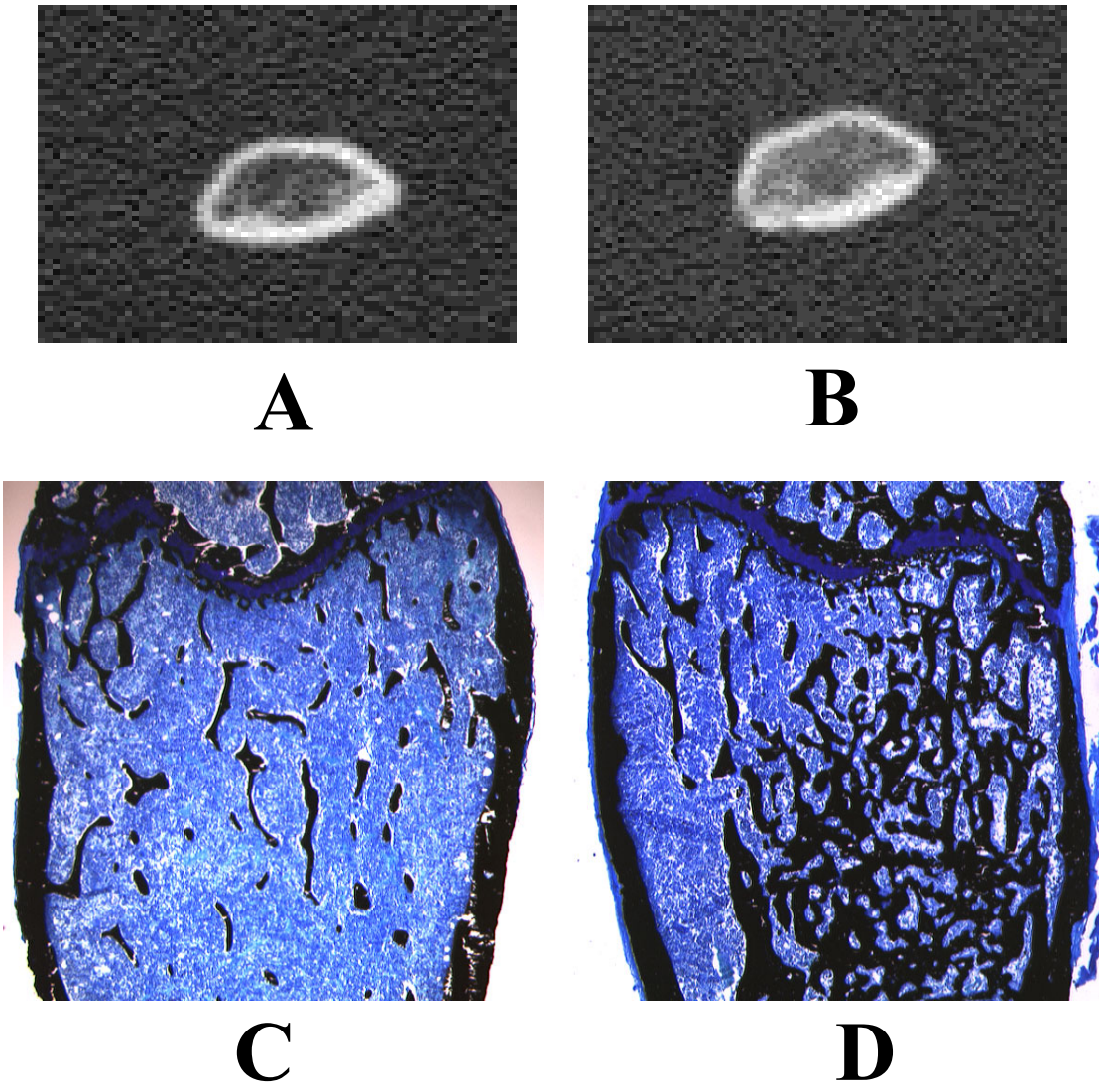

FIG. 3. Images of ablation-induced increases in cancellous bone. Distal femur metaphyses images of non-ablated control (A,C) and 10 days post-ablation (B,D) from peripheral quantitative computed tomography (pQCT; A-B) and histology (C-D). pQCT images were obtained at 3.0 mm from the distal femoral plateau using a scanning resolution of 0.07 x 0.07 x 0.50 mm. Histological sections (4 μm) were stained using the Von Kossa protocol and imaged at a magnification of 40X.

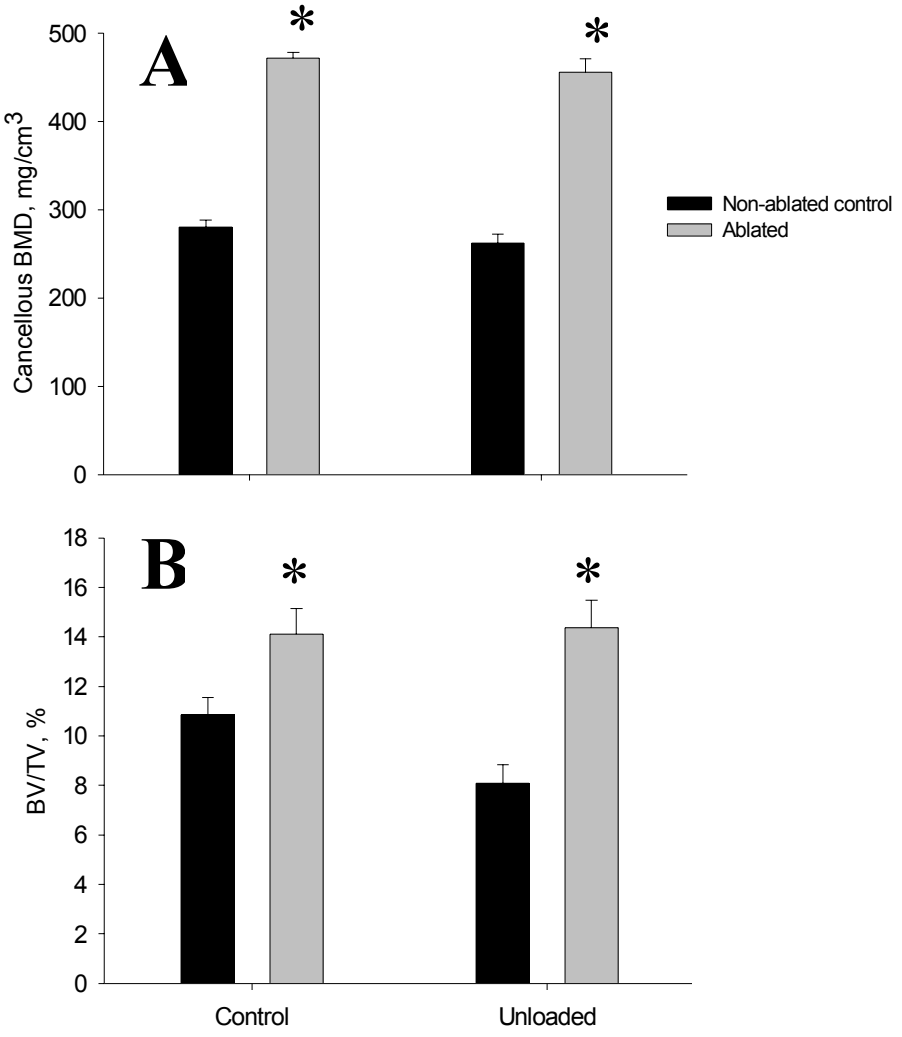

Figure 4: Ablation-induced changes in cancellous bone density and volume in loaded and unloaded animals. Cancellous bone mineral density assessed by peripheral quantitative computed tomography (A) and bone volume assessed by histology (B). Ablated limb data represent values pooled from 10 and 14 day post-ablation. Pooled group n's = 12-16. BMD, bone mineral density; BV/TV, bone volume per tissue volume. * denotes $p < 0.05$ vs. non-ablated control within group.

limb BMD values in CCAB and HUAB mice. Cancellous BMC was also significantly higher while marrow area was significantly lower in both loaded and unloaded ablated animals compared to non-ablated controls (**Table 5**); total area inside the periosteal perimeter was not different among groups.

Ablated limb cancellous BV/TV was significantly higher than non-ablated values in both control (BC: 10.9 ± 0.7; CCAB: 14.1 ± 1 %) and unloaded groups (HU: 8.1 ± 0.8; HUAB: 14.4 ± 1.1 %) with no interaction between ablation and loading (**Figure 3C-D and 4B**). Percent osteoblast surface (BC: 3.13 ± 0.5; CCAB: 7.44 ± 1.0; HU: 1.63 ± 0.4; HUAB: 6.19 ±1.2 %) and MAR (BC: 2.1 ± 0.1; CCAB: 3.5 ± 0.2; HU: 1.9 ± 0.1 HUAB: 3.6 ± 0.2 μm/day) were similarly higher in ablated control and unloaded animals as compared to the non-ablated groups (**Figure 5A, 5C**). There was no interaction of ablation and loading. Percent mineralizing surface (MS/BS) was significantly influenced by load, with unloaded animals having lower values compared to controls (**Figure 5B**); there was no significant effect of ablation in either group. There was a significant interaction between ablation and load with respect to bone formation rate (BFR). Ablated limb BFR in CCAB animals (102 ± 12 $\mu m^3/\mu m^2$/day) was nearly two-fold higher compared to that in non-ablated controls (55 ± 7 $\mu m^3/\mu m^2$/day) while there was no difference between non-ablated HU and HUAB animals (38 ± 9 and 47 ± 8 $\mu m^3/\mu m^2$/day, respectively) (**Figure 5D**). Additionally, CCAB values were significantly higher than those of HUAB animals.

Results from study two document that cbfa1 mRNA expression, relative to baseline controls, was significantly reduced at day 1 and 3 after marrow ablation with no

TABLE 5: EFFECT OF UNLOADING AND ABLATION ON PQCT PARAMETERS

	Control	AB	Control	AB
	Control		Unloaded	
BMC, mg/mm	0.29 ± 0.02	0.36 ± 0.01 *	0.24 ± 0.01	0.33 ± 0.02 *
Total area, mm^2	2.36 ± 0.12	2.40 ± 0.08	2.20 ± 0.05	2.40 ± 0.06
Marrow area, mm^2	0.99 ± 0.06	0.76 ± 0.02 *	0.87 ± 0.04	0.76 ± 0.04 *

Distal femoral metaphysis parameters assessed by peripheral quantitative computed tomography (pQCT). Data are mean ± SE of n = 12-16 animals per group, pooled from 10 and 14 day post-ablation time points. AB, marrow ablation; BMC, bone mineral content. Total area denotes all area encompassed by periosteal surface. Marrow area denotes area within the endocortical surface. * denotes significant main effect of ablation compared to non-ablated ($p < 0.05$).

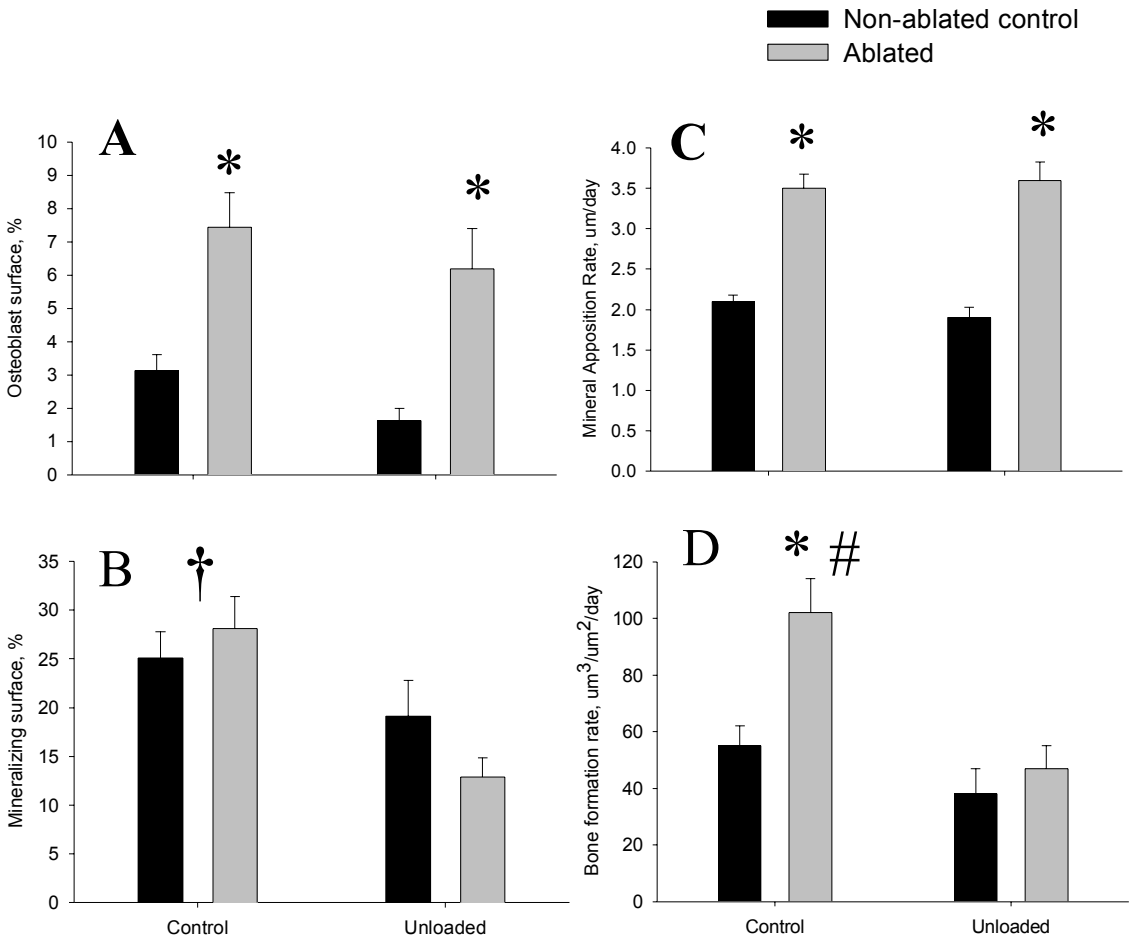

Figure 5: Ablation-induced changes in osteoblast related parameters in loaded and unloaded animals. Histologically assessed osteoblast surface (A), mineralizing surface (B), mineral apposition rate (C) and bone formation rate (D). Ablated limb data represent values pooled from 10 and 14 day post-ablation (total n = 12-16). All data refer to cancellous bone. * denotes $p < 0.05$ compared to non-ablated control within group. # denotes $p < 0.05$ vs. ablated unloaded value. † denotes $p < 0.05$ vs. unloaded when ablated and non-ablated groups are pooled.

interaction of time and treatment (**Figure 6A**). Osteocalcin mRNA expression was unchanged compared to baseline at time points measured (**Figure 6B**).

Effect of prior unloading on response to ablation. Cancellous BMC, BMD, BV/TV and MAR were significantly higher, while MS/BS and marrow area were significantly lower, in ablated bones compared to non-ablated controls (**Table 6)**. There was no difference between HUAB and HU10AB groups for these parameters. While Ob.S was significantly increased in both HUAB and HU10AB ablated limbs with respect to non-ablated animals, the magnitude of this response to ablation was different with respect to the timing of ablation (**Figure 7**). HUAB ablated limbs had a significantly greater Ob.S (6.19 ± 1.2 %) compared to HU10AB ablated limbs (3.95 ± 0.4 %). BFR values were not different among the groups (**Table 6**). Results from study two revealed that unloading prior to ablation (HU10AB groups) did not have a significant effect on relative expression of steady state cbfa1 and osteocalcin mRNA at any post-ablation time point as compared to HUAB (**Table 7**).

Discussion

The data presented herein document that weightbearing is not necessary for ablation-induced increases of osteogenic activity (e.g. bone volume and osteoblast surface). These similar increases in select osteoblast-related parameters exist despite the independent negative effects of hindlimb unloading in these skeletally mature C3H male mice. The absence of mechanical load does, however, significantly influence the mineralization of newly formed bone, suggesting that this last phase of new bone formation may be limiting during periods of disuse. In addition, when osteoblast

TABLE 6: INFLUENCE OF ABLATION TIMING ON RESPONSE IN UNLOADED BONE

	HUAB		HU10AB	
	Control	AB	Control	AB
BMC, mg/mm	0.24 ± 0.01	0.33 ± 0.02 *	0.27 ± 0.02	0.37 ± 0.02 *
BMD, mg/cm^3	276 ± 10	443 ± 11 *	262 ± 10	456 ± 15 *
Marrow area, mm^2	0.87 ± 0.04	0.76 ± 0.04 *	0.99 ± 0.05 #	0.83 ± 0.04 *
BV/TV, %	8.1 ± 0.7	14.4 ± 1.1 *	6.6 ± 0.6	12.9 ± 1.3 *
MS/BS, %	19 ± 4	13 ± 2 *	23 ± 2	20 ± 8 *
MAR, μm/day	1.9 ± 0.1	3.6 ± 0.2 *	1.9 ± 0.1	3.4 ± 0.2*
BFR, μm^3/μm^2/day	38 ± 9	47 ± 8	47 ± 6	65 ± 8

Distal femoral metaphysis parameters assessed by peripheral quantitative computed tomography (BMC/BMD) and histology (all others). Data are mean ± SE of n = 12-16 animals per group, pooled from 10 and 14 day post-ablation time points. HUAB, hindlimb unloaded with marrow ablation on day 0; HU10AB, hindlimb unloaded with marrow ablation after 10 days. BMC, bone mineral content; BMD, bone mineral density; BV/TV, bone volume per tissue volume; MS/BS, mineralizing surface per bone surface; MAR, mineral apposition rate; BFR, bone formation rate. Marrow area defined as area within the endocortical surface. All data refer to cancellous bone. * denotes overall significant effect of ablation compared to non-ablated ($p < 0.05$). # denotes significantly different from non-ablated HUAB control ($p < 0.05$).

TABLE 7: RELATIVE MRNA EXPRESSION IN UNLOADED ABLATED ANIMALS

	HUAB			HU10AB		
	1	3	10	1	3	10
Cbfa1, relative expression	0.50 ± 0.27	0.43 ± 0.29	0.63 ± 0.28	0.55 ± 0.22	0.11 ± 0.03	4.2 ± 3.8
OC, relative expression	0.65 ± 0.27	0.35 ± 0.12	1.00 ± 0.54	1.80 ± 0.78	0.40 ± 0.11	0.86 ± 0.29

Ablation-induced changes in steady state core binding factor 1 (cbfa1) and osteocalcin (OC) mRNA expression in study 2 animals sacrificed 1, 3, or 10 days after ablation. Total RNA (1μg) from isolated femora (n=4-6/gp) was reverse transcribed to cDNA and then amplified using real time PCR. Amplification was normalized to 18S RNA and values are expressed relative to BC expression levels. HUAB, hindlimb unloaded + marrow ablation on day 0; HU10AB, hindlimb unloaded for 10 days prior to marrow ablation.

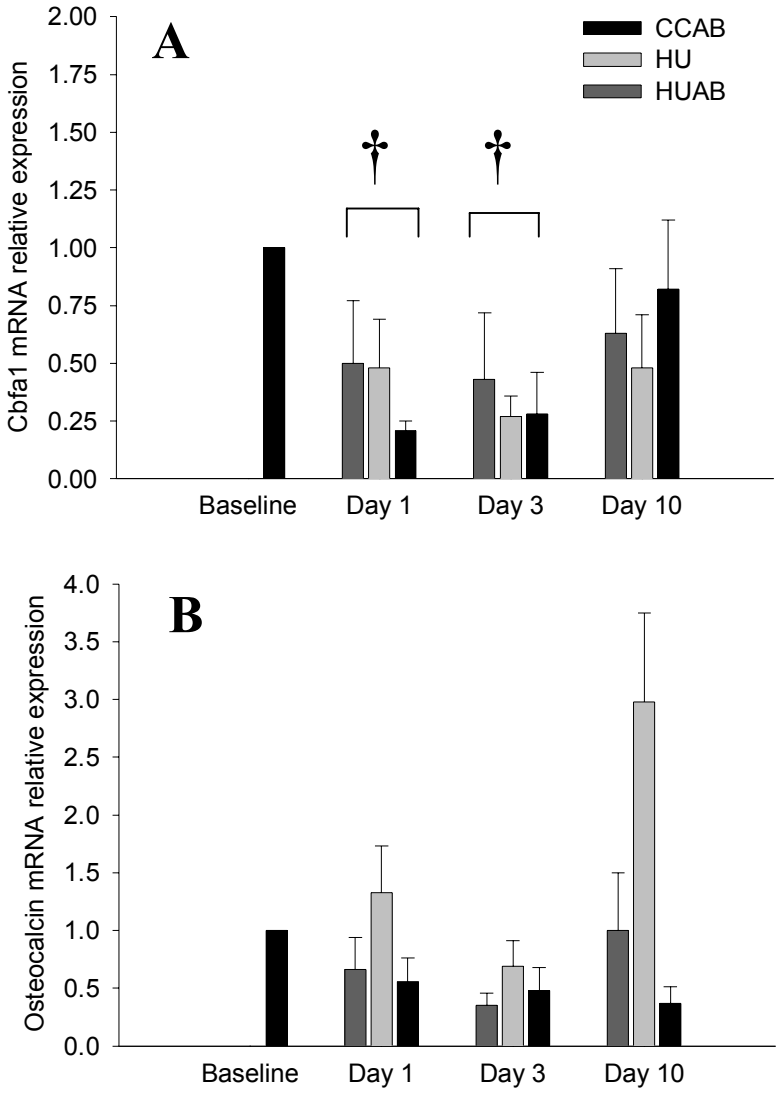

FIG. 6. Ablation-induced changes in steady state cbfa1 and osteocalcin mRNA expression. Study 2 animals sacrificed 1, 3, or 10 days after ablation. Total RNA (1µg) from isolated femora (n=4-6/gp) was reverse transcribed to cDNA and then amplified using real time PCR for cbfa1 (A) and osteocalcin (B). Amplification was normalized to 18S RNA and values are expressed relative to BC levels. † denotes $p < 0.05$ vs. baseline control when all groups in time are pooled.

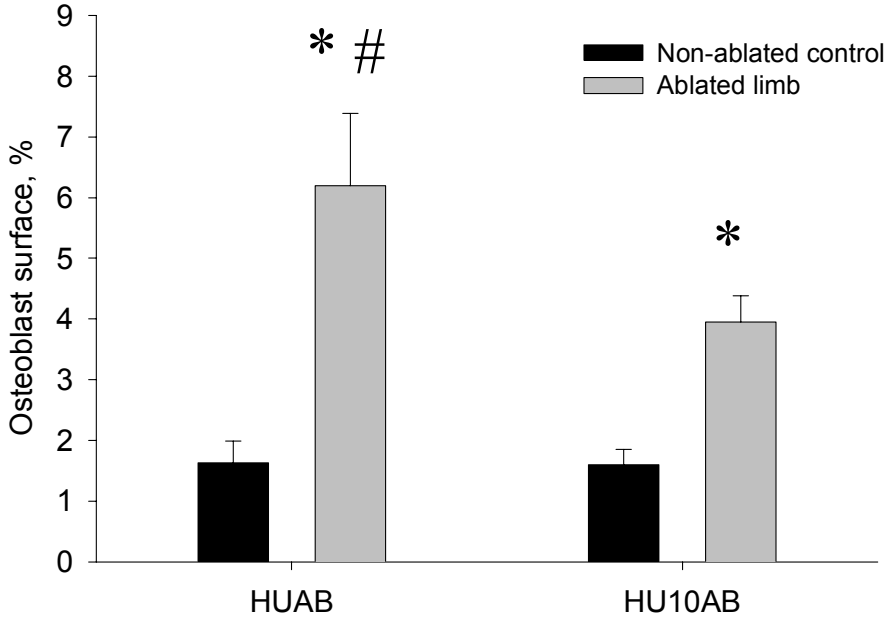

FIG. 7. Influence of ablation timing on osteoblast number in unloaded bone. Ablated limb data represent values pooled from 10 and 14 day post-ablation (total n's = 12-16). HUAB, hindlimb unloaded with marrow ablation on day 0; HU10AB, hindlimb unloaded with marrow ablation after 10 days. * denotes $p < 0.05$ vs. non-ablated control within group. # denotes $p < 0.05$ vs. ablated unloaded value.

functionality was reduced prior to ablation, the amount of osteoblast forming surface was reduced, along with the amount of mineralization. Collectively, these data document normal ablation-induced increases of cancellous bone volume even in the absence of mechanical loading. However, differences in the extent of actively mineralizing surface suggest that mineralization deficits are a major contributor to bone formation limitations during disuse.

In response to hindlimb unloading (without ablation), the skeletally mature C3H male mouse experienced significant reductions in cancellous bone volume and percent osteoblast surface. These changes occurred despite no significant change in cancellous BMD (by pQCT), percent mineralizing surface, mineral apposition rate and bone formation rate, although all statistical analyses had less than optimal power due to the large number of groups. As no study to date has assessed changes in unloaded mice using pQCT, it is not clear if the lack of cancellous BMD change with unloading is unique to the C3H strain, known for its high bone density (92), or if the resolution of pQCT scans (70μm) was not adequate to detect subtle changes in cancellous BMD of mice after this period of unloading.

Histological assessments of murine cancellous bone changes with unloading have only recently been performed using skeletally mature C3H mice (97,100). After 14 days of unloading proximal tibia cancellous bone volume in female C3H mice is lower than in controls (-31%)(100), quantitatively similar to changes observed in the distal femur metaphysis in the current study (-31% after 24 days). However, in male C3H mice no change in femoral cancellous bone volume after 14 and 21 days of unloading is noted

(97). Mineral apposition and bone formation rates do not change (female C3H)(100) or increase (male C3H)(97) compared to weightbearing controls; neither study quantified percent osteoblast surface, a variable sensitive to unloading in the current study.

These previous results, combined with the current data, suggest only a transient decrease in dynamic bone formation parameters in the skeletally mature C3H mouse with unloading. The explanation for this is unclear. Previous data suggest C3H mice may be insensitive to mechanical load perturbations, as they exhibit no increase in cortical bone formation rate compared to other strains in response to mechanical loading (115, 116). This theory does not appear to apply to cancellous bone in the current study. Significant changes with unloading are noted in select dynamic parameters when data are pooled from ablated and non-ablated animals, thus increasing the subject number and therefore the power of the analysis. However, the changes appear to be transient with respect to these dynamic parameters. Similar transient decrease in mineral apposition and bone formation rates have previously been noted when young, skeletally immature rats are unloaded (71). Thus, whether these transient decrements in dynamic cancellous properties of C3H mice are due to a lack of skeletal maturity at 4 months of age, a partial resistance to altered mechanical load, or some other factor necessitates more detailed study.

Marrow ablation, a potent bone formation stimulus, resulted in significantly higher distal femur metaphysis cancellous BMC, BMD and bone volume in both weightbearing and unloaded animals. Ablation-induced increases in femoral metaphysis bone volume have previously been quantified in weightbearing animals using microCT

(109,117) and histology (105,106). These are the first data to document that these responses will occur even in the absence of mechanical loading. The ablation-induced increase in pQCT-measured BMD, calculated as bone mineral content per unit marrow area (within the endocortical perimeter), could be accounted for by 1) an increased volume of cancellous tissue; 2) an increased density of pre-existing cancellous tissue; 3) minimal change in cancellous tissue and/or density with a concomitant decrease in marrow area or 4) a combination of all three processes. As bone mineral content within the marrow cavity was significantly increased (+35%), similar in magnitude to the increase in histologically measured bone volume (BV/TV, +33%), it is clear that ablation results in an increased volume of cancellous tissue. However, a significant decrease in marrow area was also quantified (+ 18%) suggesting that some combination of these two changes accounts for the increase in ablated animal BMD. One additional factor potentially contributing to increase density is the degree of tissue mineralization, a variable not directly quantifiable by pQCT. Thus, it is possible that subtle differences exist in the contribution of changes in bone volume, area and unmeasured parameters, such as tissue mineralization, between loaded and unloaded ablated animals.

Although unloading did not significantly reduce percent mineralizing surface in the analysis of HU only animals, there was a significant overall effect of unloading (-40%) when ablated and non-ablated limb data were pooled. This discrepancy is likely due to the low power of the HU only analysis. Previous studies have documented mineralization deficits of cortical bone formed during unloading (71,74) and spaceflight (118) in young rats, as well as during fracture healing in space-flown and hindlimb

unloaded rats (119). Only indirect evidence exists with respect to alterations of cancellous bone mineralization with unloading (120). Yet, as unloading results in highly unorganized collagen matrix (121), and this matrix directly facilitates mineralization (122), it seems reasonable to speculate that the woven bone formed in response to ablation is altered with unloading. While these deficits in mineralization must be confirmed through further study, the potential implications are significant with respect to compromised strength of bone formed during disuse.

Reductions of cancellous bone mineralizing surface in unloaded ablated mice were consistently coupled with an increased mineral apposition rates (MAR). Changes in MAR can be somewhat misleading, as this variable yields no information about the extent of surfaces with double labeling. Therefore, percent mineralizing surface and percent osteoblast surface provide a more global view of activity across all cancellous bone surfaces. Yet, these two parameters do not change in tandem, as ablation produced significant increases in percent osteoblast surface in both loaded and unloaded animals with no effect of ablation on mineralizing surface in either ablated group compared to non-ablated controls. While there is undoubtedly some temporal relationship between mineralizing and osteoblast surface, the discrepancy between these variables in unloaded ablated animals suggests a potential osteoblast dysfunction. Osteoblasts cultured in the absence of gravity exhibit reduced functionality (13) and increased apoptosis (123). Thus, osteoblasts covering cancellous bone surfaces in unloaded ablated bones may have had altered functionality (e.g. produced un-mineralizable matrix) or had increased rates of apoptosis, accounting for the discrepancy of osteoblast and mineralizing surfaces. It

can not be discounted; however, that mineralization may simply be delayed in unloaded animals.

The paradoxical lack of BFR increase in unloaded ablated bones, despite a significant increase in cancellous bone volume, is difficult to explain. Neither measure assesses the degree to which the bone that is present is mineralized, while measures of bone volume require only a minimal mineralization level to be detected. Hence, if under mineralized bone is present in unloaded animals, as suggested by pQCT results, it is possible that no increase in bone formation rate will be detected, as fluorochrome labels are only deposited on actively mineralizing surface. It should also be noted that dynamic measures assess only the activity within the final week before animal sacrifice; thus, bone formation may have been higher in unloaded ablated animals at earlier time points post-ablation before declining by the last week of the experiment.

Due to the effect of unloading and ablation on osteoblasts, mRNA levels of two osteoblast-specific markers, core binding factor 1 (cbfa1) and osteocalcin (OC) were assessed using real time PCR in an attempt to elucidate mechanisms of altered osteoblast functionality. This technique measures fluorescence emitted from amplicon-specific probes during cDNA amplification, normalized to an endogenous control (18S) amplified under identical conditions in order to account for differences in total RNA added to each reaction. Real time PCR provides certain advantages over traditional PCR, such as the ability to detect changes during the exponential growth phase rather then at the end of amplification, thus increasing the sensitivity of detection (124).

In the present study, there was a significant decrease in the expression of cbfa1 mRNA at days one and three with no difference among groups, suggesting that both unloading and ablation result in similar reductions of osteoblast differentiation signals. The fact that lower cbfa1 mRNA levels do not coincide with declines in percent osteoblast surface, at least on ablated cancellous bone surfaces, suggest that fully differentiated osteoblasts may be recruited to the marrow cavity in response to ablation. Thus, rather than relying on differentiation and proliferation of locally available osteoblast progenitors, ablation may signal peripheral osteoblasts to migrate to the area due to the need to produce cancellous bone very rapidly. It is also possible that changes in marrow cbfa1 mRNA expression were not detectable when whole bone samples were analyzed, which included bone as well as marrow. Gene expression analysis of marrow extracts may have provided different results yet separating out marrow tissue from ablated bones poses numerous problems and difficulties.

Neither ablation nor unloading significantly altered osteocalcin mRNA expression in the current study suggesting no change in functional activity of mature osteoblasts. Similar to cbfa1, these data contradict histological assessment of percent osteoblast cancellous bone surface yet lend support to the speculation regarding dysfunctional osteoblasts with ablation. Furthermore, the data obtained from PCR analysis provides information on only mRNA expression, one step in the process of producing proteins. Thus alterations in osteocalcin protein, the functional product, may be altered despite no effect on mRNA expression.

When marrow ablation was performed after a period of unloading of sufficient duration to suppress select cancellous bone parameters before ablation, BMC, BMD, bone volume and mineral apposition rate values elevated as much as those in mice unloaded on the day of ablation. Mineralizing surface of unloaded animals (independent of when ablation occurred) is significantly lower compared to non-ablated unloaded animals. When mineralizing surface data are combined with mineral apposition rate, no difference was noted among groups with respect to the rate of bone formation. These data are consistent with earlier speculation about reduced mineralization in unloaded bone, and document a further reduction in actively mineralizing surface when ablation occurs in bone already experiencing mechanical unloading. The most sensitive parameter to unloading appears to be percent osteoblast surface, as the significant increase in this parameter in HUAB animals is attenuated when bone is unloaded for ten days prior to ablation (HU10AB). This suggests a disruption in the responsiveness to anabolic stimuli if applied to bone that has been compromised by unloading. The potential implications of these results are substantial, as they suggest that countermeasures aimed at maintaining osteoblast function during disuse must be initiated very soon after disuse begins. Significant delays may compromise the efficacy of the intervention in terms of stimulating osteoblast function.

Although the series of osteogenic events following ablation are accelerated in comparison to those induced by other mechanical and pharmacological stimuli, as well as during *de novo* bone formation, the sequence of cellular events are all similar. These include increases of osteoblast surface, mineral apposition rate and bone formation rate,

eventually leading to increased bone volume. The main differences with respect to the marrow ablation model are the rapidity of the response. This unique characteristic allows the assessment of limitations in osteoblast function in an acute timeframe. Reductions of mineralization in unloaded animals have been previously documented using the fracture healing model, another extreme bone formation stimulus (119). Together, these results suggest impaired mineralization of newly formed cancellous bone in the absence of mechanical loading. As both marrow ablation and fracture healing are powerful stimuli, potentially effecting osteoblast/mineralization via unique mechanisms, these results should be confirmed using less potent bone formation stimuli such as mechanical loading or intermittent parathyroid hormone (PTH) treatment.

In conclusion, these data suggest subtle yet significant effects of unloading on the response to marrow ablation, providing insight into limitations of bone formation in the absence of mechanical load. The unique effect of unloading is with respect to a reduction in mineralizing surface, leading to an attenuation of the bone formation rate increase noted in weightbearing controls. This suggests that the limitations of bone formation with unloading are the result of altered osteoblast products (e.g. osteoid) rather than in the inability of osteoblasts to be recruited or develop normally. The caveat, however, is that when bone formation is stimulated after a period of unloading sufficient to compromise osteoblast functionality, increases in osteoblast recruitment to the bone surface are compromised.

CHAPTER IV

SUMMARY AND FUTURE RESEARCH

The goal of this project was to begin identifying the mechanisms responsible for decreased bone formation during disuse. To do so, the potent bone formation stimulus of marrow ablation was superimposed on hindlimb unloaded mice to elucidate if the ablation-induced response would occur under conditions that normally reduce osteoblast activity. These data document that ablation-induced cancellous bone exhibits mineralization deficits resulting in a failure to increase bone formation rate. The potential implication of this mineralization deficit is that bone produced in the absence of loading would have lower overall strength. This would increase the subsequent risk of fracture, especially upon the return to normal loading. Additionally, the degree of osteoblast response is sensitive to osteoblast functionality at the time of ablation. This finding significantly impacts on countermeasure initiation. If bone formation stimulation protocols are delayed for a period of time after disuse begins, the efficacy will be compromised.

While these results provide support for deficits in cancellous bone mineralization in the absence of mechanical load, many questions remain. Future studies should focus on confirming these results using 1) alternative bone formation stimuli, 2) a larger animal model, and 3) additional techniques.

The extreme nature of the marrow ablation stimulus may not have allowed the detection of subtle differences with respect to bone formation parameters between weightbearing and unloaded animals. As such, other stimuli, such as pharmacological

doses of intermittent PTH , FGF, or mechanical loading may provide additional information with respect to limitations of osteoblasts in unloaded bone. Although the mouse provides many advantages in research, there are also notable disadvantages. Due to the distinct differences in skeletal phenotypes and responses to manipulation, the responses documented herein can not be generalized beyond the C3H strain. The size of mouse bones also is prohibitive with respect to more in-depth analyses of osteoprogenitor cells confined to the marrow. For these reasons, the use of rats may be advantageous although there are also disadvantages using this species such as the longer timeframe to reduce osteoblast functionality (~ 21 days). Finally, additional techniques should be used to further investigate limitations in mineralization with unloading. This is probably most easily accomplished through culture of the ablated limb bone marrow at various time points following ablation, focusing specifically on mineralization outcomes. Based on these cell culture results further analyses could focus on specific factors (genes, transcription factors, cytokines, hormones) which contribute to the decrements in mineralization. Techniques in addition to cell culture may include imagining methods such as quantitative backscattered electron imaging, synchrotron radiation microtomography, scanning small angle X-ray scattering, Fourier transform infrared microspectroscopy, and Raman spectroscopy. These methods provide data on the degree of mineralization in discrete bone regions as well as mineral structure and composition, therefore potentially providing a means to more completely assess how mineralization is altered in the absence of mechanical loads.

REFERENCES

1. Rubin C, Lanyon L 1984 Regulation of bone formation by applied dynamic loads. J Bone Joint Surg Am **66:**397-402.
2. Ball J, Evans Jr C 2001 Safe passage. Astronaut care for exploration missions, First ed. National Academy Press, Washington DC, pp 291.
3. Morey-Holton E, Globus R 2002 Invited review: Hindlimb unloading rodent model: technical aspects. J Appl Physiol **92:**1367-1377.
4. Aubin J, Triffitt J 2002 Mesenchymal stem cells and osteoblast differentiation. In: Bilezikian J, Raisz L, Rodan G (eds.) Principles of bone biology, 2nd ed., vol. 1. Academic Press, San Diego, pp 59-81.
5. Dennis J, Charbord P 2002 Origin and differentiation of human and murine stroma. Stem Cells **20:**205-214.
6. Aubin J 1998 Bone stem cells. J Cell Biochem **30-31:**73-82.
7. Rodan G 1998 Control of bone formation and resorption: biological and clinical perspective. J. Cell Biochem **30-31:**55-61.
8. Schinke T, Karsenty G 2002 Transcriptional control of osteoblast differentiation and function. In: Bilezikian J, Raisz L, Rodan G (eds.) Principles of bone biology, vol. 1. Academic Press, San Diego, pp 83-91.
9. Lian J, Stein G, Canalis E, Robey P, Boskey A 1999 Bone formation: Osteoblast lineage cells, growth factors, matrix proteins, and the mineralization process. In:

Favus M (ed.) Primer on the metabolic bone diseases and disorders of mineral metabolism, Fourth ed. Lippincott Williams & Wilkins, Philadelphia, pp 14-29.

10. Aubin J 2001 Regulation of osteoblast formation and function. Rev Endo Met Dis **2:**81-94.
11. Carmeliet G, Bouillon R 1999 The effect of microgravity on morphology and gene expression of osteoblasts in vitro. FASEB J. **13:**S129-S134.
12. Hughes-Fulford M, Lewis M 1996 Effects of microgravity on osteoblast growth activation. Exp Cell Res **224:**103-109.
13. Hughes-Fulford M 2001 Changes in gene expression and signal transduction in microgravity. J Gravit Physiol **81:**1-4.
14. Carmeliet G, Nys G, Stockmans I, Bouillon R 1998 Gene expression related to the differentiation of osteoblastic cells is altered by microgravity. Bone **22:**139S-143S.
15. Carmeliet G, Nys G, Bouillon R 1997 Microgravity reduced the differentiation of human osteoblastic MG-63 cells. J Bone Miner Res **125:**786-794.
16. Kumei Y, Akiyama H, Hirano M, Shimokawa H, Morita S, Mukai C, Nagaoka S 1999 Space flight modulates signal transduction pathway of growth factor receptors in rat osteoblasts. Biol Sci Space **13:**142-143.
17. Fitzgerald J, Hughes-Fulford M 1996 Gravitational loading of a simulated launch alters mRNA expression in osteoblasts. Exp Cell Res **228:**168-171.
18. Ontiveros C, McCabe L 2003 Simulated microgravity suppresses osteoblast phenotype, Runx2 levels and AP-1 transactivation. J Cell Biochem **88:**427-437.

19. Narayanan R, Smith C, Weigel N 2002 Vector-averaged gravity-induced changes in cell signaling and vitamin D receptor activity in MG-63 cells are reversed by 1,25-(OH)2D3 analog, EB1089. Bone **31:**381-388.

20. Rucci N, Migliaccio S, Zani B, Taranta A, Teti A 2002 Characterization of the osteoblast-like cell phenotype under microgravity conditions in the NASA-approved Rotating Wall Vessel bioreactor (RWV). J Cell Biochem **85:**167-179.

21. Arnaud S, Sherrard D, Maloney N, Whalen R, Fung P 1992 Effects of 1-week head-down tilt bed rest on bone formation and the calcium endocrine system. Aviat Space Environ Med **63:**14-20.

22. Deitrick J, Whedon G, Shorr E 1948 Effects of immobilization upon various metabolic and physiologic functions of normal men. Am J Med **99:**716-731.

23. van der Wiel H, Lips P, Nauta J, Netelenbos J, Hazenberg G 1991 Biochemical parameters of bone turnover during ten days of bed rest and subsequent mobilization. Bone Miner **13:**123-129.

24. Issekutz B, Blizzard J, Birkhead N, Rodahl K 1966 Effect of prolonged bed rest on urinary calcium output. J Appl Physiol **21:**1013-1020.

25. Schneider V, McDonald J 1984 Skeletal calcium homeostasis and countermeasures to prevent disuse osteoporosis. Calcif Tissue Int **36:**S151-S154.

26. Scheld K, Zittermann A, Heer M, Herzog B, Mika C, Drummer C, Stehle P 2001 Nitrogen metabolism and bone metabolism markers in healthy adults during 16 weeks of bed rest. Clin Chem **47:**1688-1695.

27. Zerwekh J, Ruml L, Gottschalk F, Pak C 1998 The effects of twelve weeks of bed rest on bone histology, biochemical markers of bone turnover, and calcium homeostasis in eleven normal subjects. J Bone Miner Res **13:**1594-1601.

28. Donaldson C, Hulley S, Vogel J, Hattner R, Bayers J, McMillan D 1970 Effects of prolonged bed rest on bone mineral. Metabolism **19:**1071-1084.

29. LeBlanc A, Schneider V, Evans H, Engelbretson D, Krebs J 1990 Bone mineral loss and recovery after 17 weeks of bed rest. J Bone Miner Res **5:**843-850.

30. Uebelhart D, Bernard J, Hartmann D, Moro L, Roth M, Uebelhart B, Rahailia M, Mauco G, Schmitt D, Alexandre C, Vico L 2000 Modifications of bone and connective tissue after orthostatic bedrest. Osteoperos Int **11:**59-67.

31. LeBlanc A, Schneider V, Krebs J, Evans H, Jhingran S, Johnson P 1987 Spinal bone mineral after 5 weeks of bed rest. Calcif Tissue Int **41:**259-261.

32. Mack P, LaChance P 1967 Effects of recumbency and space flight on bone density. Am J Clin Nut **20:**1194-1205.

33. Lueken S, Arnaud S, Taylor A, Baylink D 1990 Immobilization causes an acute and sustained increase in markers of bone resorption. Clin Res **38:**123.

34. LeBlanc A, Schneider V, Spector E, Evans H, Rowe R, Lane H, Demers L, Lipton A 1995 Calcium absorption, endogenous excretion, and endocrine changes during and after long-term bed rest. Bone **16:**301S-304S.

35. Inoue M, Tanaka H, Moriwake T, Oka M, Sekiguchi C, Seino Y 2000 Altered biochemical markers of bone turnover in humans during 120 days of bed rest. Bone **26:**281-286.

36. Smith S, Nillen J, LeBlanc A, Lipton A, Demers L, Lane H, Leach C 1998 Collagen cross-link excretion during space flight and bed rest. J Clin Endocrinol Metab **83:**3584-3591.

37. Lueken S, Arnaud S, Taylor A, Baylink D 1993 Changes in markers of bone formation and resorption in a bed rest model of weightlessness. J Bone Miner Res **8:**1433-1438.

38. Palle S, Vico L, Bourrin S, Alexandre C 1992 Bone tissue response to four-month antiorthostatic bedrest: a bone histomorphometric study. Calcif Tissue Int **51:**189-194.

39. Vico L, Chappard D, Alexandre C, Palle S, Minaire P, Riffat G, Morukov B, Rakhmanov S 1987 Effects of a 120 day period of bed-rest on bone mass and bone cell activities in man: attempts at countermeasure. Bone Miner **2:**383-394.

40. Hattner R, McMillan E 1968 Influence of weightlessness upon the skeleton: a review. Aero Med **39:**849-855.

41. Rambaut P, Johnston R 1979 Prolonged weightlessness and calcium loss in man. Acta Astro **6:**1113-1122.

42. Vogel J, Whittle M 1976 Bone mineral changes: the second manned Skylab mission. Aviat Space Environ Med **47:**396-400.

43. Rambaut P, Smith M, Mack P, Vogel J Ranbayt P 1975 Skeletal Results. In: Pool S, Parker J, Jones W (eds.) Biomedical results of Apollo, Washington DC: NASA.

44. Reid J, Lutwak L, Whedon G 1968 Dietary control in metabolic studies of Gemini-7 space flight. J Am Diet Assoc **53:**342-347.

45. Whedon G, Lutwak L, Rambaut P, Whittle M, Smith M, Reid J, Leach C, Stadler C, Sanford D 1977 Mineral and nitrogen metabolic studies, experiment M071. In: Johnson R, Dietlein L (eds.) Biomedical Results from Skylab NASA SP-377, Washington, DC: NASA, p. 164-174.

46. Smith S, Wastney M, Morukov B, Larina I, Nyquist L, Abrams S, Taran E, Shih C, Nillen J, Davis-Street J, Rice B, Lane H 1999 Calcium metabolism before, during, and after a 3-mo spaceflight: kinetic and biochemical changes. Am J Physiol **277**(Regul Integr Comp Physiol)**:**R1-R10.

47. Caillot-Augusseau A, Lafage-Prouse M, Soler C, Pernod J, Dubois F, Alexandre C 1998 Bone formation and resorption biological markers in cosmonauts during and after a 180-day space flight (Euromir 95). Clin Chem **44:**578-85.

48. Stupakov G, Kazeikin V, Kozlovskii A, Korolev V 1984 Evaluation of changes in human axial skeletal bone structure during long-term spaceflights. Space Biol Med **18:**42-47.

49. Collet P, Uebelhart D, Vico L, Moro L, Hartmann D, Roth M, Alexandre C 1997 Effects of 1- and 6-month spaceflight on bone mass and biochemistry in two humans. Bone **20:**547-551.

50. Vico L, Collet P, Guignandon A, Lafage-Proust M, Thomas T, Rehaillia M, Alexandre C 2000 Effects of long-term microgravity exposure on cancellous and cortical weight-bearing bones of cosmonauts. Lancet **355:**1607-1611.

51. Mack P 1971 Bone density changes in a Macaca nemestrina monkey during the biosatellite 3 project. Aero Med **42:**828-833.

52. Zerath E, Novikov V, LeBlanc A, Bakulin A, Oganov V, Grynpas M 1996 Effects of spaceflight on bone mineralization in the rhesus monkey. J Appl Physiol **81:**194-200.

53. Oganov V, Bakulin A, Novikov V, Murashko L 2000 Changes and recovery of bone mass and acoustic properties of rhesus monkeys after Bion 11 spaceflight. J Gravit Physiol **7:**S163-S168.

54. Zerath E, Holy X, Andre C, Renault S, Noel B, Delannoy P, Hott M, Marie P 2000 Effects of Bion 11 14-day space flight on monkey iliac bone. J Gravit Physiol **7:**S155-S156.

55. Arnaud S, Navidi M, Deftos L, Thierry-Palmer M, Dotsenko R, Bigbee A, Grindeland R 2002 The calcium endocrine system of adolescent rhesus monkeys and controls before and after spaceflight. Am J Physiol **282**(Endo Metab)**:**E514-E521.

56. Zerath E, Grynpas M, Holy X, Viso M, Patterson-Buckendahl P, Marie P 2002 Spaceflight affects bone formation in rhesus monkeys: a histological and cell culture study. J Appl Physiol **93:**1047-1056.

57. Rodionova N, Shevel I, Oganov V, Novikov V, Kabitskaya O 2000 Bone ultrastructural changes in Bion 11 rhesus monkeys. J Gravit Physiol **7:**S157-S161.

58. Yagodovsky Y, Triftanidi L, Gorokhova G 1976 Space flight effects on skeletal bones of rats (light and electron microscopic examination). Aviat Space Environ Med **47:**734-738.

59. Cavolina J, Evans G, Harris S, Zhang M, Westerlind K, Turner R 1997 The effects of orbital spaceflight on bone histomorphometry and messenger ribonucleic acid levels for bone matrix proteins and skeletal signaling peptides in ovariectomized growing rats. Endocrinology **138:**1567-1576.

60. Jee W, Wronski T, Morey E, Kimmel D 1983 Effects of spaceflight on trabecular bone in rats. Am J Physiol **244:**R310-R314.

61. Vico L, Chappard D, Palle S, Bakulin A, Novikov V, Alexandre C 1988 Trabecular bone remodeling after seven days weightlessness exposure (BIOCOSMOS 1667). Am J Physiol **225**(Reg Integ Comp Physiol)**:**R243-R247.

62. Vico L, Bourrin S, Genty C, Palle S, Alexandre C 1993 Histomorphometric analyses of cancellous bone from COSMOS 2044 rats. J Appl Physiol **75:**2203-2208.

63. Zerath E, Godet D, Holy X, Andre C, Renault S, Hott M, Marie P 1996 Effects of spaceflight and recovery on rat humeri and vertebrae: histological and cell culture studies. J Appl Physiol **81:**164-171.

64. Zerath E, Holy X, Roberts S, Andre C, Renault S, Hott M, Marie P 2000 Spaceflight inhibits bone formation independent of corticosteroid status in growing rats. J Bone Miner Res **15:**1310-1320.

65. Wronski T, Morey-Holton E, Doty S, Maese A, Walsh C 1987 Histomorphometric analysis of rat skeleton following spaceflight. Am J Physiol **252**(Reg Int Comp Physiol)**:** R252-R255.

66. Turner R, Evans G, Wakley G 1995 Spaceflight results in depressed cancellous bone formation in rat humeri. Aviat Space Environ Med **66:**770-774.

67. Roberts W, Mozsary P 1981 Suppression of osteoblast differentiation during weightlessness. Physiologist **24:**S75-S76.

68. Bikle D, Harris J, Halloran B, Morey-Holton E 1994 Altered skeletal pattern of gene expression in response to spaceflight and hindlimb elevation. Am J Physiol **267:**E822-E827.

69. Evans G, Morey-Holton E, Turner R 1998 Spaceflight has compartment- and gene-specific effects on mRNA levels for bone matrix proteins in rat femur. J Appl Physiol **84:**2132-2137.

70. Morey E 1979 Spaceflight and bone turnover: Correlation with a new rat model of weightlessness. BioSci **29:**168-172.

71. Globus R, Bikle D, Morey-Holton E 1986 The temporal response of bone to unloading. Endocrinology **118:**733-742.

72. Bikle D, Morey-Holton E, Doty S, Currier P, Tanner S, Halloran B 1994 Alendronate increases skeletal mass of growing rats during unloading by inhibiting resorption of calcified cartilage. J Bone Miner Res **9:**1777-1787.

73. Halloran B, Bikle D, Harris J, Tanner S, Curren T, Morey-Holton E 1997 Regional responsiveness of the tibia to intermittent administration of parathyroid hormone as affected by skeletal unloading. J Bone Miner Res **12:**1068-1074.

74. Globus R, Bikle D, Morey-Holton E 1984 Effects of simulated weightlessness on bone mineral metabolism. Endocrinology **114:**2264-2270.

75. Machwate M, Zerath E, Holy X, Hott M, Godet D, Lomri A, Marie P. 1995 Systemic administration of transforming growth factor-beta 2 prevents the impaired bone formation and osteopenia induced by unloading in rats. J Clin Invest **96:**1245-1253.

76. Barou O, Lafage-Proust M, Martel C, Thomas T, Tirode F, Laroche N, Barbier A, Alexandre C, Vico L 1999 Bisphosphonate effects in rat unloaded hindlimb bone loss model: three-dimensional microcomputed tomographic, histomorphometric, and densitometric analyses. J Pharmacol Exp Ther **291:**321-328.

77. Ahdjoudj S, Lasmoles F, Holy X, Zerath E, Marie P 2002 Transforming growth factor-beta 2 inhibits adipocyte differentiation induced by skeletal unloading in rat bone marrow stroma. J Bone Miner Res **17:**668-677.

78. Grano M, Mori G, Minielli V, Barou O, Colucci S, Giannelli G, Alexandre C, Zallone A, Vico L 2002 Rat hindlimb unloading by tail suspension reduces osteoblast differentiation, induces IL-6 secretion, and increases bone resorption in ex vivo cultures. Calcif Tissue Int **70:**176-185.

79. Barou O, Palle S, Vico L, Alexandre C, Lafage-Proust M 1998 Hindlimb unloading in rat decreases preosteoblast proliferation assessed in vivo with BrdU incorporation. Am J Physiol **274**(Am J Physiol Endo Metab)**:**E108-E114.

80. Vico L, Bourrin S, Novikov V, JM. V, Chappard D, Alexandre C 1991 Adaptation of bone cellular activities to tail suspension in rats. Cells Materials **1:**143-150.

81. Wronski T, Morey E 1982 Skeletal abnormalities in rats induced by simulated weightlessness. Metab Bone Dis Relat Res **4:**69-75.

82. Fielder P, Morey E, Roberts W 1986 Osteoblast histogenesis in periodontal ligament and tibial metaphysis during simulated weightlessness. Aviat Space Environ Med **57:**1125-30.

83. Kostenuik P, Halloran B, Morey-Holton E, Bikle D 1997 Skeletal unloading inhibits the in vitro proliferation and differentiation of rat osteoprogenitor cells. Am J Physiol **273:**E1133-E1139.

84. Zhang R, Supowit S, Klein G, Lu Z, Christensen M, Lozano R, Simmons D 1995 Rat tail suspension reduces messenger RNA levels for growth factors and osteopontin and decreases the osteoblastic differentiation of bone marrow stromal cells. J Bone Miner Res **10:**415-423.

85. Kimmel D 1991 Quantitative histologic changes in the proximal tibial growth cartilage of aged female rats. Cells Materials **1:**11-18.

86. Dehority W, Halloran B, Bikle D, Curren T, Kostenuik P, Wronski T, Shen Y, Rabkin B, Bouraoui A, Morey-Holton E 1999 Bone and hormonal changes

induced by skeletal unloading in the mature male rat. Am J Physiol **276:**E62-E69.

87. Vico L, Bourrin S, Very J, Radziszowska M, Collet P, Alexandre C 1995 Bone changes in 6-mo-old rats after head-down suspension and a reambulation period. J Appl Physiol **79:**1426-1433.

88. Bloomfield S, Allen M, Hogan H, Delp M 2002 Site- and compartment-specific changes in bone with hindlimb unloading in mature adult rats. Bone **31:**149-157.

89. Rubin C, Xu G, Judex S 2001 The anabolic activity of bone tissue, suppressed by disuse, is normalized by brief exposure to extremely low-magnitude mechanical stimuli. FASEB J. **15:**2225-2229.

90. Cowin S 2001 Bone mechanics handbook, Second ed. CRC Press, Boca Raton, FL.

91. Thomas T, Lafage-Proust M 1999 Contributions of genetically modified mouse models to the elucidation of bone physiology. Rev Rhum Eng Ed **62:**728-735.

92. Beamer W, Donahue L, Rosen C, Baylink D 1996 Genetic variability in adult bone density among inbred strains of mice. Bone **18:**397-403.

93. Akhter M, Iwaniee U, Covey M, Cullen D, Kimmel D, Recker R 2000 Genetic variations in bone density, histomorphometry, and strength in mice. Calcif Tissue Int **67:**337-344.

94. Ortoft G, Andreassen T, Oxlund H 1999 Growth hormone increases cortical and cancellous bone mass in young growing rats with glucocorticoid-induced osteopenia. J Bone Miner Res **14:**710-721.

95. Simske S, Luttges M, Allen K, Gayles E 1994 The role of sex and genotype on antiorthostatic suspension effects on the mouse peripheral skeleton. Aviat Space Environ Med **65:**123-33.

96. Bateman T, Broz J, Fleet M, Simske S 1998 Differing effects of two-week suspension on male and female mouse bone metabolism. Biomed Sci Instrum **34:**374-379.

97. Amblard D, Lafage-Proust M, Laib A, Thomas T, Ruegsegger P, Alexandre C, Vico L 2003 Tail suspension induces bone loss in skeletally mature mice in the C57BL/6J strain but not in the C3H/HeJ strain. J Bone Miner Res **18:**561-569.

98. Sakai A, Nakamura T 2001 Changes in trabecular bone turnover and bone marrow cell development in tail-suspended mice. J Musculoskel Neuron Interact **1:**387-392.

99. Rantakokko J, Uusitalo H, Jamsa T, Tuukkanen J, Aro H, Vuorio E 1999 Expression profiles of mRNAs for osteoblast and osteoclast proteins as indicators of bone loss in mouse immobilization osteopenia model. J Bone Miner Res **14:**1934-1942.

100. Judex S, Donahue L, Rubin C 2002 Genetic predisposition to low bone mass is paralleled by an enhanced sensitivity to signals anabolic to the skeleton. FASEB J. **16:**1280-1282.

101. Amsel S, Maniatis A, Tavassoli M, Crosby W 1969 The significance of intramedullary cancellous bone formation in the repair of bone marrow tissue. Anat Rec **16:**101-111.

102. Patt H, Maloney M 1975 Bone marrow regeneration after local injury: a review. Exp Hematol **3:**135-148.

103. Suva L, Seedor J, Endo N, Quartuccio H, Thompson D, Bab I, Rodan G 1993 Pattern of gene expression following rat tibial marrow ablation. J Bone Miner Res **8:**379-388.

104. Gazit D, Karmish M, Holzman L, Bab I 1990 Regenerating marrow induces systemic increase in osteo- and chondrogenesis. Endocrinology **126:**2607-2613.

105. Liang C, Barnes J, Seedor J, Quartuccio H, Bolander M, Jeffrey J, Rodan G 1992 Impaired bone activity in aged rats: alterations at the cellular and molecular levels. Bone **13:**435-441.

106. Marusic A, Grcevic D, Katavic V, Kovacic N, Lukic I, Kalajzic I, Lorenzo J 2000 Role of B lymphocytes in new bone formation. Lab Invest **80:**1761-1774.

107. Bab I, Gazit D, Massarawa A, Sela J 1985 Removal of tibial marrow induces increased formation of bone and cartilage in rat mandibular condyle. Calcif Tissue Int **37:**551-555.

108. Tanaka H, Barnes J, Liang C 1996 Effect of age on the expression of insulin-like growth factor-I, interleukin-6, and transforming growth factor-beta mRNAs in rat femurs following marrow ablation. Bone **18:**473-478.

109. Shimizu T, Mehdi R, Yoshimura Y, Yoshikawa H, Nomura S, Miyazono K, Takaoka K 1998 Sequential expression of bone morphogenetic protein, tumor necrosis factor, and their receptors in bone-forming reaction after mouse femoral marrow ablation. Bone **23:**127-133.

110. Iris B, Zilberman Y, Zeira E, Galun E, Honigman A, Turgeman G, Clemens T, Gazit Z, Gazit D 2003 Molecular imaging of the skeleton: quantitative real-time bioluminescence monitoring gene expression in bone repair and development. J Bone Miner Res **18:**570-578.

111. Ishijima M, Tsuji K, Rittling S, Yamashita T, Kurosawa H, Denhardt D, Nifuji A, Noda M 2002 Resistance to unloading-induced three-dimensional bone loss in osteopontin-deficient mice. J Bone Miner Res **17:**661-667.

112. Chen X, Allen M, Bloomfield S, Xu T, Young M 2003 Biglycan-deficient mice have delayed osteogenesis after marrow ablation. Calcif Tissue Int (In press).

113. Parfitt A, Drezner M, Glorieux F, Kanis J, Malluche H, Meunier P, Ott S, Recker R 1987 Bone histomorphometry: standardization of nomenclature, symbols, and units. J Bone Miner Res **2:**595-610.

114. Livak K, Schmittgen T 2001 Analysis of relative gene expression data using real-time quantitative PCR and the 2(-Delta Delta C(T)) method. Methods **254:**402-8.

115. Kadoma Y, Umermura Y, Nagasawa S, Beamer W, Donahue L, Rosen C, Baylink D, Farley J 2000 Exercise and mechanical loading increases periosteal bone formation and whole bone strength in C57BL/6J mice but not in C3H/Hej mice. Calcif Tissue Int **66:**298-306.

116. Pedersen E, Akhter M, Cullen D, Kimmel D, Recker R 1999 Bone response to in vivo mechanical loading in C3H/HeJ mice. Calcif Tissue Int **65:**41-46.

117. Yamashita T, Yoshitake H, Tsuji K, Kawaguchi N, Nabeshima Y, Noda M 2000 Retardation in bone resorption after bone marrow ablation in klotho mutant mice. Endocrinology **141:**438-445.

118. Turner R, Bell N, Duvall P, Bobyn J, Spector M, Morey-Holton E, Baylink D 1985 Spaceflight results in formation of defective bone. Proc Soc Exp Biol Med **180:**544-549.

119. Kaplansky A, Durnova G, Burkovskaya T, Vorotnikova E 1991 The effect of microgravity on bone fracture healing in rats flown on Cosmos-2044. Physiologist **32:**S196-199.

120. Allen M, Hogan H, Weigel N, Bloomfield S 1,25-dihydroxyvitamin D_3 and its analog, EB1089, differentially benefit cancellous and cortical bone mechanical properties in skeletally mature hindlimb unloaded rats. J Bone Miner Res (In review).

121. Shiiba M, Arnaud S, Tanzawa H, Kitamura E, Yamauchi M 2002 Regional alterations of type I collagen in rat tibia induced by skeletal unloading. J Bone Miner Res **17:**1639-1645.

122. Boskey A, Wright T 1999 Collagen and bone strength. J Bone Miner Res **143**:330-335.

123. Rucci N, Migliaccio S, Zani B, Taranta A, Teti A 2002 Characterization of the osteoblast-like cell phenotype under microgravity conditions in the NASA-approved rotating wall vessel bioreactor (RWV). J Cell Biochem **85**:167-179.

124. Bustin S 2002 Quantification of mRNA using real-time reverse transcription PCR (RT-PCR): trends and problems. J Mol Endo **29:**23-39.

VITA

Matthew Robert Allen

602 Riverside, Clare, MI 48617

EDUCATION

B.S: Exercise and Health Science, May 1998, Alma College, Alma MI.
PhD: Kinesiology, Texas A&M University, August 2003, College Station TX.

PROFESSIONAL ASSOCIATIONS

American College of Sports Medicine (1998-)
Board of Trustees Student Trustee 2002-2004
Student Affairs Committee Chair 2001-2003
Texas American College of Sports Medicine (1998-)
Board of Directors Student Representative 1999-2001
American Society of Bone and Mineral Research (1998-)
American Physiological Society (1999-)
International Bone and Mineral Society (2000-)

PUBLISHED MANUSCRIPTS

SA Bloomfield, MR Allen, HA Hogan, and MD Delp. Site- and compartment-specific changes in bone with hindlimb unloading in mature adult rats. Bone 31:1 149-57.

MR Allen and SA Bloomfield. Cancellous bone maintenance following long-term hindlimb unloading in skeletally mature female rats. J Appl Physiol 94: 642-650, 2003.

XD Chen, MR Allen, S Bloomfield, T Xu, and M Young. Biglycan Deficient Mice Have Delayed Osteogenesis after Marrow Ablation. CTI (In press 2003).

AWARDS AND HONORS

Texas ACSM Doctoral Poster Award (2nd place), 2002
Sun Valley Hard Tissue Workshop Young Investigator Travel Award, 2001
Texas ACSM Manuscript Award (2nd place), 2001
Texas ACSM Doctoral Poster Award (2nd place), 2000
Texas A&M Student Research Week Biological Science Oral Presentation, Doctoral category, 2000